Marine and Petroleum Geology 142 (2022) 105757

Contents lists available at ScienceDirect

Marine and Petroleum Geology

journal homepage: www.elsevier.com/locate/marpetgeo

Organic-rich, fine-grained contourites in an epicontinental basin: The Upper Jurassic-Lower Cretaceous Vaca Muerta Formation, Argentina

Maximiliano Paz [a,*], Luis A. Buatois [a], M. Gabriela Mángano [a], Patricio R. Desjardins [b], Raúl Notta [b], Federico González Tomassini [c], Noelia B. Carmona [d,e], Daniel Minisini [f,g]

[a] University of Saskatchewan, Department of Geological Sciences, 114 Science Place, S7N 5E2, Saskatoon, Canada
[b] Shell Exploration and Production Company, 150N Dairy Ashford St, TX, 77019, Houston, USA
[c] Phoenix Global Resources, Alem 855, C1001AAQ, Buenos Aires, Argentina
[d] Universidad Nacional de Río Negro, Instituto de Investigación en Paleobiología y Geología, General Roca, Argentina
[e] Instituto de Investigación en Paleobiología y Geología (IIPG), CONICET, Av. J. A. Roca 1242, 8332, General Roca, Argentina
[f] Shell Technology Center Houston, 3333 South HW 6, TX, 77082, Houston, USA
[g] Department of Earth, Environmental and Planetary Sciences, Rice University, Houston, TX, USA

ARTICLE INFO

Keywords:
Unconventional reservoir
Fine-grained depositional systems
Oxygen
Bioturbation
Traction structures
Neuquén basin

ABSTRACT

Over the last few years, recognition and characterization of sedimentary processes in fine-grained successions is receiving considerable attention in part due to the increased importance of unconventional reservoirs. Recent sedimentologic analyses of these successions have revealed abundant traction transport structures that suggest bottom current activity of different origins. The present study constitutes a detailed sedimentologic analysis of the Upper Jurassic-Lower Cretaceous Vaca Muerta Formation (Neuquén Basin, Argentina), which comprises organic-rich, fine-grained subaqueous clinoform deposits. Locally, intervals showing traction structures such as parallel lamination, ripple cross-lamination and cross-bedding, and displaying high bioturbation, occur. These intervals can be differentiated into three facies associations, namely crinoidal mixed to calcareous mudstone, mixed to calcareous mudstone, and calcareous to mixed mudstone interbedded with calcareous mudstone. These facies associations were deposited by contour currents showing semi-permanent activity, low sediment concentration, and generating long-term oxygen supply to the seafloor. Locally, some successions display an increasing to decreasing bioturbation intensity pattern that may have a similar origin to the bi-gradational sequence of contourites. The present sedimentologic analysis supports the idea that contour currents are associated with high bioturbation levels due to increased oxygenation, which controls the degree of preservation of traction structures, and consequently the possibility to delineate these processes in fine-grained successions. These currents occurred in relatively shallow water, probably as part of a weakened estuarine or anti-estuarine, basin-wide circulation system intensified by the enhanced action of dense water cascading during arid and cool climate periods.

1. Introduction

Contour currents represent processes that occur in open oceans (Flemming, 1980, 1981; Ramsay, 1994; Viana et al., 1998a, 2002; Liu et al., 2006) and epicontinental basins (Sivkov et al., 2002; Cattaneo et al., 2003; Verdicchio and Trincardi, 2008a; Vandorpe et al., 2011; Pellegrini et al., 2016; Moros et al., 2020), associated with wind- and thermohaline-induced circulation. Contourites are increasingly being analyzed in modern environments due to their importance for hydrocarbon exploration, paleoceanographic and paleoclimatologic studies, and assessment of slope stability (Rebesco et al., 2014; Miramontes et al., 2019; De Castro et al., 2021). However, contourites are hard to delineate in ancient successions because of the difficulty of establishing a concrete facies model. This issue stems from the complexity associated with bottom current transport ("bottom current" constitute a generic term that includes processes such as thermohaline- and wind-driven

* Corresponding author.
E-mail addresses: maxi.paz@usask.ca (M. Paz), luis.buatois@usask.ca (L.A. Buatois), gabriela.mangano@usask.ca (M.G. Mángano), p.desjardins@shell.com (P.R. Desjardins), raul-carlos.notta@shell.com (R. Notta), f.gonzalezt@phoenixgr.com (F. González Tomassini), ncarmona@unrn.edu.ar (N.B. Carmona), daniel.minisini@shell.com (D. Minisini).

https://doi.org/10.1016/j.marpetgeo.2022.105757
Received 6 June 2021; Received in revised form 16 May 2022; Accepted 18 May 2022
Available online 21 May 2022

contour currents, cascading and internal waves). For example, bottom current forcing mechanism can be mixed, precluding the usage of a precise nomenclature associated with the origin of the currents (Shanmugam, 2017). In addition, currents can interact with other processes such as turbidity flows, generating a continuum between different processes and facies (Stow and Smillie, 2020).

More than ten years have passed since the paradigm of mud accumulation shifted from fine-grained sediment deposited by fallout in low-energy environments to interpretations of more variable energetic conditions at the seafloor (Macquaker and Bohacs, 2007; Schieber et al., 2007). Traction structures, represented by silt laminae encased in mudstone and muddy ripple cross-lamination, have been observed in numerous fossil examples of fine-grained depositional systems and interpreted as produced by bottom currents of various origins (e.g., Pratt, 1984; Oczlon and Díez Balda, 1992; Schieber, 1994, 1999, 2016; O'Brien, 1996; Loucks and Ruppel, 2007; Singh et al., 2008; Trabucho-Alexandre et al., 2012; Egenhoff and Fishman, 2013; Leonowicz, 2013; Nyhuis et al., 2014; Reisdorf et al., 2014; Birgenheier et al., 2017; Li and Schieber, 2018; Minisini et al., 2018). Particularly, silt laminae structures have been reproduced in flume experiments, representing deposits created by bedload traction transport of mixed silt-mud loads (Yawar and Schieber, 2017). Documentation of ancient examples of contour currents in shallow, epicontinental seas includes the Middle and Upper Devonian of Canada (Knapp et al., 2017; Ayranci et al., 2018) and the Upper Jurassic of Texas (Frébourg et al., 2013). Most of these examples share several similarities with the fine-grained succession analyzed in this contribution: they are composed of fine-grained sediments with high organic matter content, and they were deposited in oxygen-deficient seafloors in shallow seas. However, there are still several questions regarding bottom current deposits and the associated environmental controls. For example, the role of bioturbation and oxygen supply is debated (Shanmugam, 2013), the facies model of these currents in the shallow-water realm is not well-constrained (Stow and Faugères, 2008), and the likely origin or triggering factors are relatively unknown (Schieber, 2016).

The example studied herein comes from the Vaca Muerta Formation (Neuquén Basin, Argentina, Fig. 1A and B), the hottest unconventional play outside North America (Minisini et al., 2020a). This formation represents a shallow-marine, mixed carbonate-siliciclastic muddy clinoform system developed during the Late Jurassic-Early Cretaceous (Stipanicic, 1969; Leanza, 1973). It mostly comprises mixed and calcareous mudstone, limestone and volcaniclastic beds, and is characterized by high total organic carbon (av. 3.2%, Brisson et al., 2020). Sedimentologic analyses of this formation are numerous, comprising outcrop studies (Spalletti et al., 2000; Kietzmann et al., 2014a; Zeller et al., 2015; Ponce et al., 2015; Krim et al., 2017; Paz et al., 20192021; Otharán et al., 2020) and core investigations (González Tomassini et al., 2014; Desjardins et al., 2018; Minisini et al., 2020b). In addition, sedimentologic analysis and reservoir characterization have been carried out in the cores from the study area (Pose et al., 2014; Repol et al., 2014; Notta et al., 2017, 2020; Desjardins and Aguirre, 2018; Gómez Rivarola and Borgnia, 2018; Estrada et al., 2020; Minisini et al., 2020b). Several authors have interpreted the activity of bottom currents of different origins in distal environments of the Vaca Muerta Formation from other outcrop locations (e.g. Gasparini et al., 1997; Spalletti et al., 1999; Scasso et al., 2002; Kietzmann et al., 2008, 2014a; Kietzmann and Palma, 2009a; Zeller et al., 2015; Rodríguez Blanco et al., 2020). However, a detailed sedimentologic and sequence stratigraphic analysis

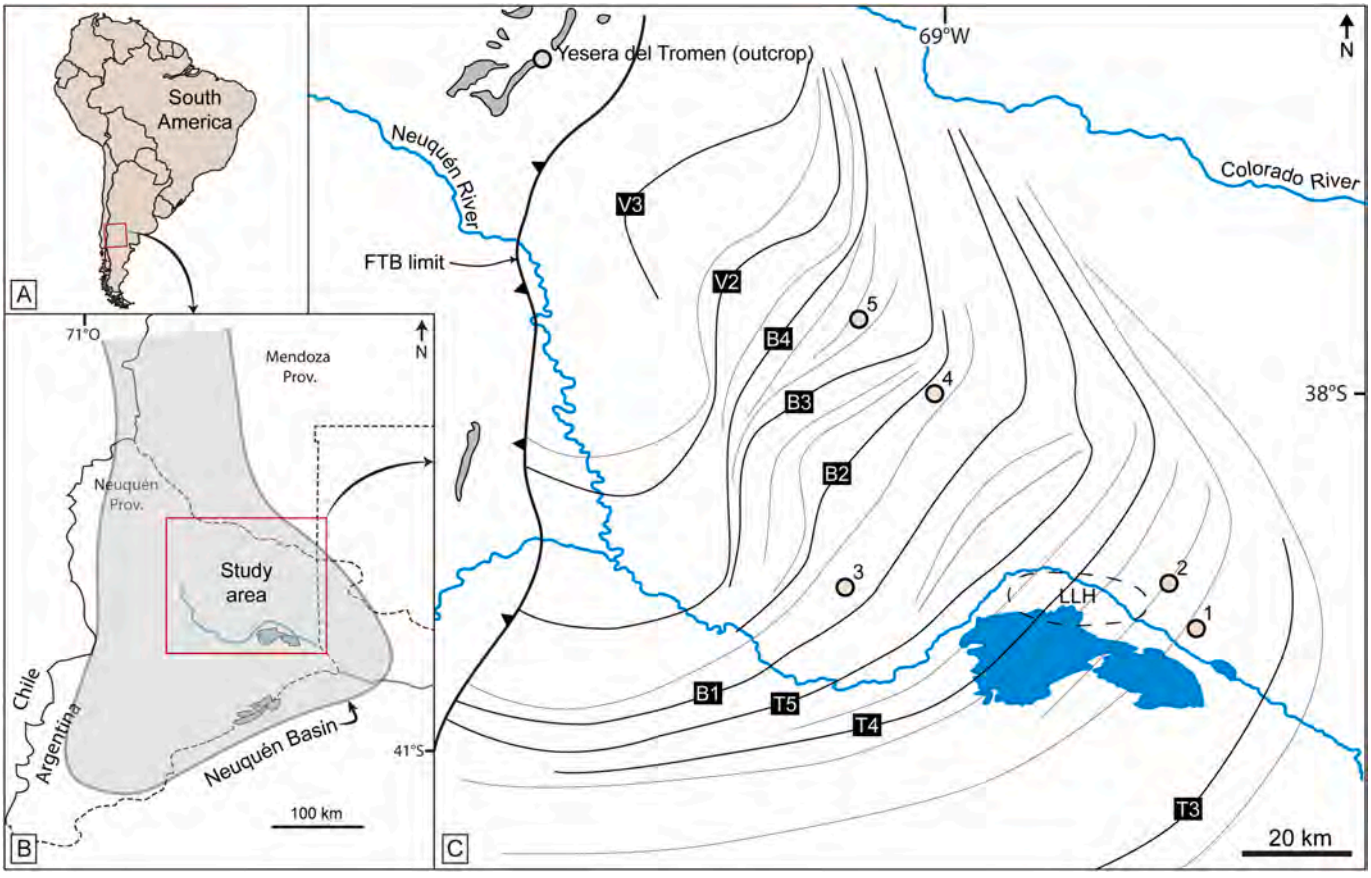

Fig. 1. Location maps (adapted from Paz et al., 2022). A, B) Map showing Neuquén Basin and study area location within a regional context. C) Study area map displaying the location of wells (1–5) and the outcrop section. Clinoform breaks from the different stratigraphic surfaces of the Vaca Muerta Formation were delineated (T2-T4, B1–B4, V2, V3; modified from Domínguez et al., 2020b). Grey areas are outcrops of the Vaca Muerta Formation, located west of the fold and thrust belt (FTB). Dashed line encloses the Loma La Lata High (LLH).

of bottom current deposits is lacking. In addition, an explanation of their origin and triggering mechanisms have been previously proposed (Zeller et al., 2015; Reijenstein et al., 2020; Rodríguez Blanco et al., 2020), yet the present analysis reviews and refines this interpretation. In this study, the analysis focuses on three facies associations displaying traction structures and variable bioturbation intensity that are interpreted to represent the action of contour currents. The objectives are to describe facies, combine it with ichnologic data to characterize facies associations, and interpret sedimentary processes and paleoecologic controls associated with contour current activity. This dataset is analyzed to explore several lines of evidence that can be used to recognize contour current activity in fine-grained depositional systems and to characterize the origin of the circulation system associated with the currents.

2. Geologic setting

2.1. Regional context

The Neuquén Basin represents a triangular-shaped depocenter whose infill history is subdivided into three stages: syn-rift, back-arc, and foreland (Howell et al., 2005; Casadío and Montagna, 2015). The first stage occurred during the Late Triassic to Early Jurassic, comprising volcaniclastic and epiclastic continental sedimentation in several rift depocenters (Carbone et al., 2011). The back-arc stage showed the establishment of Andean volcanism and extensive subsidence since the Early Jurassic, with multiple transgressions and regressions (Howell et al., 2005; Casadío and Montagna, 2015). Finally, the foreland phase started during the Late Cretaceous after the closure of the marine connection of the basin with the Pacific Ocean, and was dominated by continental sedimentation (Tunik et al., 2010).

The Vaca Muerta Formation represents a marine episode of the back-arc stage developed from late early Tithonian to early Valanginian (Leanza, 1973; Leanza et al., 2011). This formation overlies the Kimmeridgian eolian, lacustrine and fluvial deposits of the Tordillo Formation (Spalletti et al., 2011), and is capped transitionally by the upper Tithonian to early Valanginian, carbonate and siliciclastic offshore to nearshore deposits of the Quintuco Formation (Mitchum and Uliana, 1985). The Vaca Muerta-Quintuco System forms a succession of northwestward progradational clinoforms, up to 1800 m thick (Gulisano et al., 1984; Legarreta and Gulisano, 1989), subdivided into six units (Fig. 2, Desjardins et al., 2018; Minisini et al., 2020a). The system shows a very high variability throughout the basin. In the north (Mendoza Province), shallower-water facies were deposited in a ramp rich in carbonate deposits (Kietzmann et al., 2008, 2014a), whereas in the south, a higher siliciclastic composition can be observed, with the development of a mixed carbonate-siliciclastic shelf (Spalletti et al., 2000; Zeller et al., 2015; Krim et al., 2017; Paz et al., 2019).

2.2. Stratigraphic framework of the studied deposits

The study area comprises the Neuquén Embayment, the most active location in terms of hydrocarbon exploration and development (Fig. 1C). Biostratigraphic correlation using ammonites indicates that the Vaca Muerta Formation in the study area was deposited from late early Tithonian to late Tithonian-?early Berrasian (Desjardins and Aguirre, 2018; Desjardins et al., 2018). The analyzed cores were recovered from the lower three units of the Vaca Muerta-Quintuco System, where a shallow-marine mixed carbonate-siliciclastic clinoform system can be observed in seismic records (Fig. 2; Desjardins et al., 2018). Unit 1 shows the development of a low-angle clinoform system (0.2–0.3°), whereas higher angles are found in the younger units (1–3°, Minisini et al., 2020b). Core descriptions supported with Total Organic Carbon (TOC) and X-Ray Diffraction (XRD) analyses (silica, carbonate, clay ternary diagram) indicate that the lithologies are dominated by mixed (siliceous-calcareous-argillaceous) mudstone, siliceous and calcareous mudstone, limestone, and argillaceous tuffs (aka ash beds, bentonites, tefras or volcaniclastic layers; Pose et al., 2014; Repol et al., 2014; Notta et al., 2017, 2020; Desjardins and Aguirre, 2018; Gómez Rivarola and Borgnia, 2018; Minisini et al., 2020b; Reijenstein et al., 2020).

In terms of sedimentary environments, the succession in the study area encompass beach, open bay, basin, slope and contourite drift environments (Paz, 2021). The beach and open bay deposits occur at the base of the Vaca Muerta Formation, and comprise massive, parallel-, low-angle and current-ripple cross-laminated, medium-to coarse--grained sandstone with local mudstone drapes, overlain by bindstone, and massive (bioturbated) to wavy, calcareous to mixed mudstone (Paz, 2021; Paz et al., 2021).

The basin deposits are observed in bottomset to lower foreset locations of the Vaca Muerta Formation, composed by parallel-laminated, carbonaceous to bioclastic mixed mudstone, massive (bioturbated), calcareous to mixed mudstone, bioclastic floatstone to rudstone, tuff, bindstone and carbonate concretions. These deposits represent dominantly pelagic and hemipelagic sedimentation and subordinate bottom currents, sediment-gravity flows and storm events in basin environments (Paz, 2021).

The slope deposits are delineated in foreset locations, represented by parallel-to wavy-, laminated or bedded, and massive (bioturbated), calcareous to mixed mudstone, thin-bedded, massive and composite

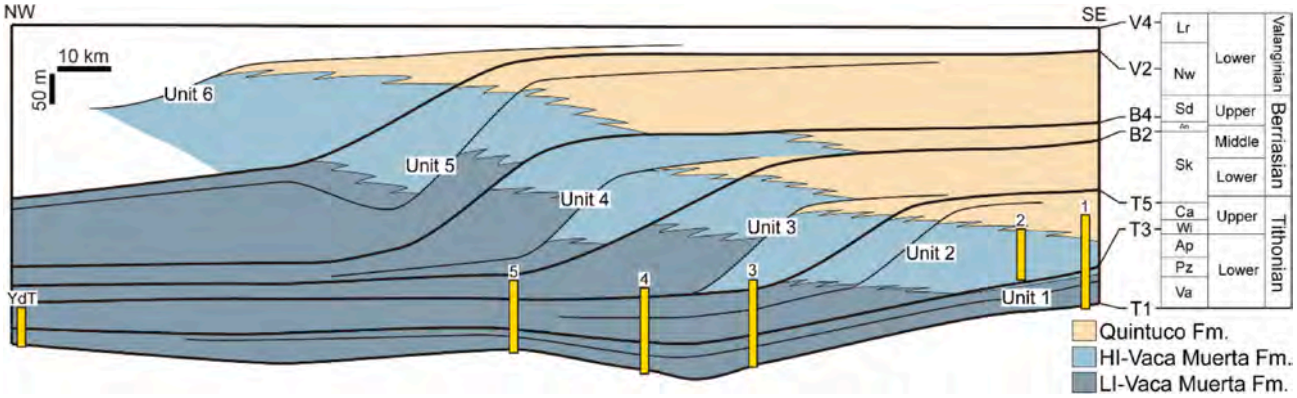

Fig. 2. Regional stratigraphic cross-section showing location of the studied cores and the Yesera del Tromen outcrop (YdT) within the Vaca Muerta-Quintuco system (adapted from Sattler et al., 2016; Reijenstein et al., 2017; Paz et al., 2022). The Vaca Muerta Formation is subdivided into a high (HI) and low (LI) impedance units. Sequence-stratigraphic surfaces (T1, T3, T5, B2, B4, V2, V4) and Units (1–6) from Desjardins et al. (2018) and Domínguez et al. (2020a, 2020b), and Andean ammonite zones (right) from Kietzmann et al. (2018). Va = *Virgatosphinctes andesensis*, Pz = *Pseudolissoceras zitteli*, Ap = *Aulacosphinctes proximus*, Wi = *Windhauseniceras internispinosum*, Ca = *Corongoceras alternans*, Sk = *Substeueroceras koeneni*, An = *Argentiniceras noduliferum*, Sd = *Spiticeras damesi*, Nw = *Neocomites wichmanni*, Lr = *Lissonia riveroi*.

		Appearence in core	Size/ grain	Bed thickness	Description	BI	Interpretation	Facies distribution
Contour current facies	$M_{cr}b$		Fine to coarse mud and crinoids	5-50 cm	Completely bioturbated intervals, with rare bedding observed. Biodeformational structures are abundant, with minor discrete trace fossils	4-6	High abundance of organisms supported by high food and oxygen availability. Hydrodynamic energy remains low and burrowing infauna keeps pace with seafloor accretion	Dominant in FA1
	$M_{cr}h$, $M_{cr}l$, $M_{cr}w$	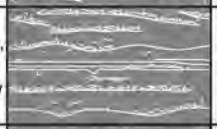	Fine to coarse mud and crinoids	2-15 cm	Discontinuous to continuous, planar, parallel-, low-angle to rare wavy-laminated crinoidal mudstone	0-3	Bedload traction transport in crinoid-rich sediments. Low-energy unidirectional currents associated with winnowing of muds	Dominant in FA1
	$M_{cr}r$	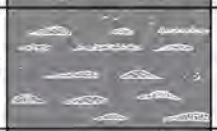	Crinoids	2-15 cm	Crinoidal mudstone with lenticular-shaped (0.5-3 mm-thick), crinoid-rich structures	0	Interpreted as starved ripples due to their common gradation from crinoid-rich laminae. Moderate energy conditions	Dominant in FA1
	$M_{cr}p$		Crinoids, peloids	5-15 cm	Cross-bedded crinoidal-peloidal mudstone with sharp to erosive bases	0	Bioclastic dune migration affected by high energy unidirectional currents	Subordinate in FA1
	$M_{cm}b$		Fine to coarse mud	1-30 cm	Completely bioturbated intervals. Some remaining bedding can be recognized. Dominant biodeformational structures and rare discrete traces are distinguished	4-5	High abundance of organisms supported by high food and oxygen availability. Hydrodynamic energy remains low and the burrowing infauna keeps pace with seafloor accretion	Dominant in FA2
	M_h, M_l		Fine to coarse mud	0.2-5 cm	Parallel to low-angle coarse mudstone laminae encased in fine mudstone	0-3	Silt and mud floccule segregation from bedload traction transport. Unidirectional currents associated with low energy and sedimentation rate	Dominant in FA2 and FA3
	M_sh, M_sl	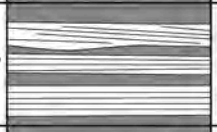	Coarse mud	0.2-5 cm	Lenticular to tabular, parallel- to low-angle cross-laminated coarse mudstone	0-3	Bedload traction transport under moderate energy and low sedimentation rate, above the threshold of mud floccule deposition	Dominant in FA2 and FA3
	M_sr, M_sw		Coarse mud to very fine-grained sand	0.2-5 cm	Lenticular to tabular, current- and wave-ripple cross-laminated coarse mudstone with black-colored laminae	0-3	Bed erosion and bedload traction transport under higher energy and sedimentation rate. Rare oscillatory current influence	Common in FA2 and FA3
	M_pl	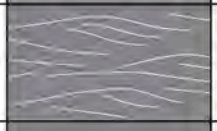	Medium to coarse mud	20-70 cm	Ripple cross-laminated peloidal mudstone associated with low-angle cross-bedded surfaces	0	Migration of compound dunes due to high-energy unidirectional currents. Possible tidal influence?	Subordinate in FA2
Sediment-gravity flow facies	M_sg, M_sm		Fine to coarse mud	0.2-20 cm	Normal-graded to massive fine to coarse mudstone with sharp bases	0-3	Normal graded beds suggesting differential settling of particles in a low-density turbidity flow. Massive beds indicative of more concentrated flows	Subordinate in FA1, FA2 and FA3
	M_cm, $M_{co}mp$		Fine to coarse mud	0.1-5 cm	Massive, calcareous medium to coarse mudstone, and composite beds of calcareous mudstone showing alternation of current-ripple cross-lamination, parallel-lamination, and normal and inverse grading	0-1	Lack of normal grading pointing towards a fluid mud flow suffering en masse deposition. Minor current ripples indicative of the existence of local turbulence within the flow	Dominant in FA3
Other facies	Tg; Tm		Coarse mud to very fine-grained sand-sized	1-20 cm	Normal-graded to massive, tuff to lapilli ash-tuff	0-1	Submarine volcanic fallout deposition and resedimented volcaniclastic deposits	Subordinate in FA1
	B_m			5-20 cm	Bindstone. Laminae with crinkly texture, composed by microsparite dolomite	0-1	Crinkled texture considered as an ancient analog of the lamination created by modern microbial mats	Subordinate in FA3

Fig. 3. Facies constituting contourite drift facies associations in the study area.

beds of calcareous mudstone, and m-thick slumped intervals. These deposits were formed by hemipelagic and fluid mud deposition below and near the storm wave-base (Paz, 2021).

The contourite drift deposits are the focus of the present study (see also Paz et al., 2022). These deposits occur in bottomset to lower foreset locations, and are characterized by massive (bioturbated), cross-bedded, parallel-, low angle- and wavy-laminated, crinoidal, mixed to calcareous mudstone, crinoid-rich lenses, parallel to low-angle, mixed to calcareous coarse mudstone laminae encased in fine mudstone, massive (bioturbated), parallel-, low-angle and current-ripple cross-laminated,

mixed to calcareous coarse mudstone, and thin-bedded, massive, normal-graded and composite beds of calcareous fine to coarse mudstone. Paleowater depth of the Vaca Muerta Formation varies between 50 and 400 m (Mitchum and Uliana, 1985; Kietzmann et al., 2008; Kietzmann and Palma, 2009a, 2009b; Minisini et al., 2020b), and thus, contourite deposits described herein can be considered mainly of shallow water (Stow et al., 1998).

Summarizing, in terms of sedimentary processes, pelagic and hemipelagic sedimentation with minor sediment-gravity flows, and bottom/contour currents affected most of the bottomset and lower foreset locations (Paz, 2021). The foreset of clinoforms is mainly developed in the study area during deposition of Unit 2, encompassing hemipelagic sedimentation, bottom/contour currents and fluid muds (Paz, 2021). The study area shows a different sedimentary evolution compared with the southern part of the basin, where higher siliciclastic influence and probably warm and humid conditions generated deposition of hyperpycnal flows in the bottomset (Krim et al., 2017; Paz et al., 2019).

3. Materials and methods

The studied material consists of cores (660.5 m) from five wells located in the Neuquén Embayment (Figs. 1C and 2). In addition, observations from the Yesera del Tromen section (148 m thick, Units 1 to 3, northern Neuquén Province) were helpful to visualize the deposits at a mesoscale. However, the sedimentologic and sequence stratigraphic analyses were based on the core data (five wells). Macroscopic observations, thin sections (59 sections from cores, 18 from outcrop samples), and mineralogic composition from XRD analysis on cores were combined to define lithology. Lithology is described following Lazar et al. (2015) for mudstone (where fine mud is < 8 μm, medium mud is 8–32 μm, and coarse mud is 32–62.5 μm), and Wright (1992) for facies rich in carbonate components. The first modifier of mudstone reflects the component (either quartz, carbonate, or clay) that is greater than 50% in the rock (Lazar et al., 2015), whereas the term "mixed mudstone" has been used for mudstone without a dominant component (<50% in abundance). The lithologic code follows the proposal of Kietzmann et al. (2014a; referring to lithology, composition, and sedimentary structures). Paleocurrent directions are not provided because geographic orientation of cores was not recorded during the recovery process. Short-wave (254 nm) and long-wave (365 nm) UV light was utilized to delineate trace fossils in black mudstone lacking sediment contrast. Bioturbation index (BI) was determined following the scheme by Taylor and Goldring (1993; modified from Reineck, 1963), which comprises a zero to six scale that considers burrow density and overlap, and preservation of bedding boundaries (percentage of bioturbated area are 1–4% for BI 1, 5–30% for BI 2, 31–60% for BI 3, 61–90% for BI 4, 91–99% for BI 5 and 100% for BI 6). Additional unpublished data available from companies owning these cores was incorporated in the analysis (i.e., electric logging data, X-Ray Fluorescence, XRD, TOC from cutting samples; see also Pose et al., 2014; Repol et al., 2014; Notta et al., 2017, 2020; Desjardins and Aguirre, 2018; Gómez Rivarola and Borgnia, 2018; Estrada et al., 2020; Minisini et al., 2020b). Redox-sensitive elements (Mo and U) were evaluated to assess paleo-oxygen levels. U enrichment was calculated following its relationship with detrital U (Wignall and Myers, 1988). A scheme of facies and facies associations was used for the sedimentologic analysis. Facies were combined with ichnologic data to define facies associations characterizing depositional environments. The sequence stratigraphic analysis follows the proposal of Hunt and Tucker (1992) and Catuneanu (2006).

4. Sedimentary facies and facies associations

The present analysis focuses on deposits showing evidence of contour current activity. Twenty-one sedimentary facies were defined (Fig. 3). These facies were subsequently clustered into three facies associations corresponding to contourite drift environments (Figs. 4 and 5, Table 1). The trace fossil data of these facies associations have been characterized in Paz et al. (2022). Geochemical data is summarized in Fig. 6.

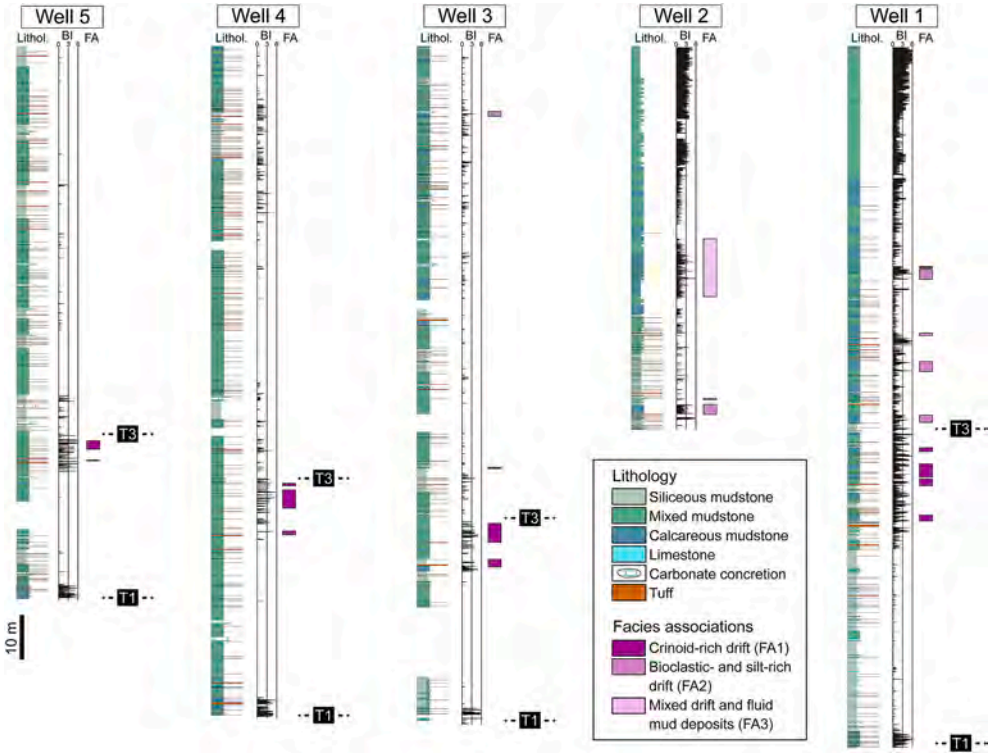

Fig. 4. Cores of the Vaca Muerta Formation with XRD analysis providing lithology, bioturbation index (BI), and facies associations (FA, adapted from Paz et al., 2022). Stratigraphic surfaces T1 and T3 define the bases of Unit 1 and Unit 2, respectively, of the Vaca Muerta-Quintuco clinoform system (Desjardins et al., 2018; Minisini et al., 2020a).

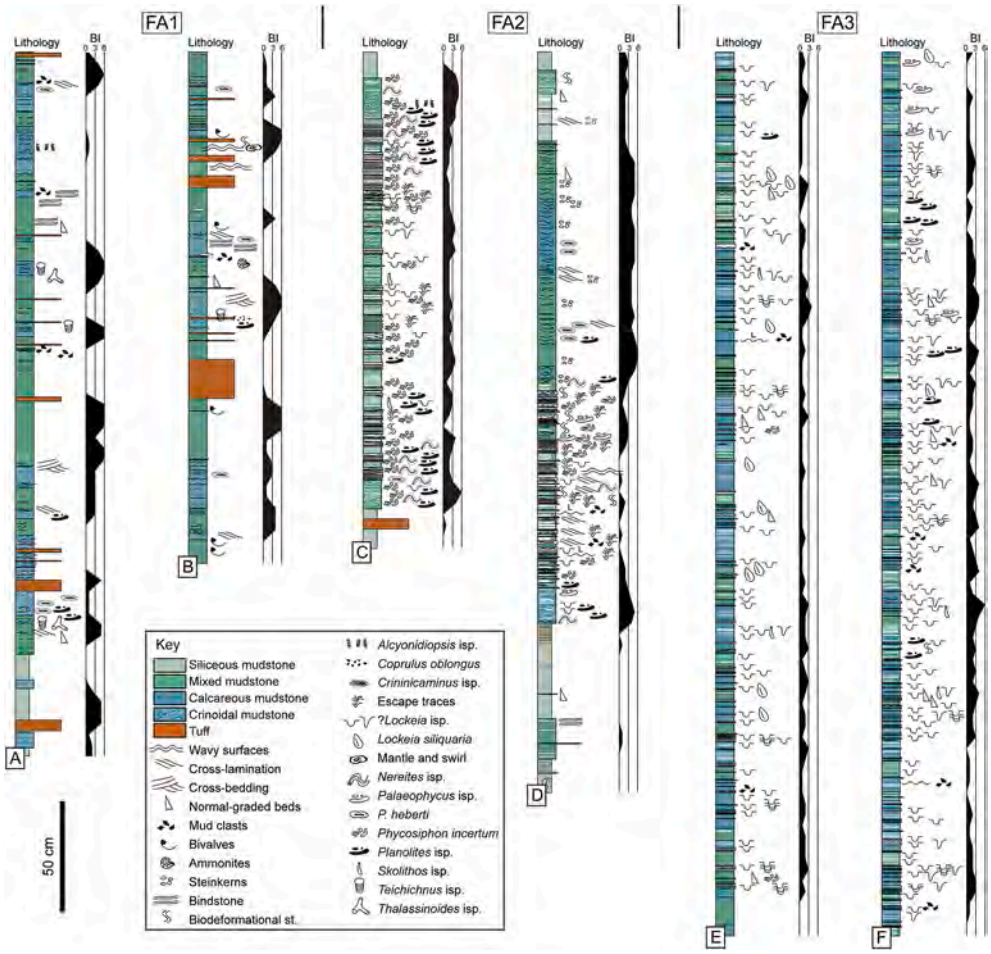

Fig. 5. Detailed stratigraphic sections of intervals containing contourite deposits. A, B) Facies association 1 from well 5. C, D) Facies association 2 from wells 1 and 2. E, F) Facies association 3 from well 2.

4.1. *Facies association 1 (FA1): crinoidal, mixed to calcareous mudstone*

4.1.1. *Description*

This facies association consists of 5–50 cm-thick, massive, mixed to calcareous crinoidal mudstone (M_{cr}b, Fig. 7A), 2-15 cm-thick, crinoidal, mixed to calcareous mudstone showing discontinuous to continuous, planar, parallel- to low-angle crinoid-rich laminae (M_{cr}h, M_{cr}l, Fig. 7B), and lenticular-shaped (0.5–3 mm thick and 2–20 mm long), crinoid-rich structures (M_{cr}r, Figs. 7B and 8A, B, C). 2-5 cm-thick, wavy-laminated crinoidal, mixed to calcareous mudstone (M_{cr}w), 5-15 cm-thick, planar cross-bedded, crinoidal, mixed to calcareous mudstone (M_{cr}p; Fig. 8D), very thin-to thin-bedded, sharp-to erosive-based, normal-graded to massive, calcareous fine to coarse mudstone (M_sg, M_sm), and thin-to thick-bedded tuff to lapilli-ash tuff (Tm, Tg), are subordinate. Facies M_{cr}b, M_{cr}h, M_{cr}l, and M_{cr}w have transitional bases, whereas facies M_{cr}r and M_{cr}p show sharp to erosive bases. Laminae are 1–2 mm thick. Average TOC is 4.04% (N = 8, Fig. 6B). The fossil content predominantly includes *Saccocoma* microcrinoids showing random orientations (Fig. 9A), with minor ammonites and bivalves. Facies M_{cr}b and M_{cr}p consist of loosely to densely packed (20–50%), fragmented to well-preserved (0.5–5 mm long) microcrinoids, whereas facies M_{cr}h, M_{cr}l, M_{cr}w and M_{cr}r show densely packed (90–100%) fragmented (<2 mm diameter) microcrinoids. In thin section, the facies association displays silt-sized radiolarians, plagioclase, quartz, and volcanic rock fragments.

Bioturbation intensity is high in M_{cr}b (BI = 3–6), and absent or low in the rest of the facies (BI = 0–1). Biodeformational structures are the most abundant biogenic structures, being locally associated with *Crininicaminus* isp. and *Planolites* isp., and rare *Teichichnus rectus, Phycosiphon incertum*, ?*Skolithos* isp., *Coprulus oblongus* and *Thalassinoides* isp.

4.1.2. *Interpretation*

This facies association is interpreted as the product of semi-permanent contour currents in areas rich in pelagic crinoids (*Saccocoma*, Kietzmann and Palma, 2009b). The lenticular structures in M_{cr}r are interpreted as starved ripples due to their common gradation from lenticular structures to laminae (Fig. 7C) and their erosive bases. The starved ripples and bioclastic laminae (M_{cr}h, M_{cr}l, M_{cr}w) indicate bed-load traction transport and winnowing of muds. In addition, bioclastic lineation in an element map core image is observed in similar facies (Gómez Rivarola and Borgnia, 2018, their fo3.4.b), supporting the traction transport hypothesis. Facies M_{cr}p suggests bioclastic dune migration. In other areas, the pelagic crinoids have been interpreted as suspension feeders (Hess and Etter, 2011), indicating the existence of continuous currents that maintained food in suspension and suggesting an active circulation system. High bioturbation intensity in M_{cr}b indicates oxygenated environments, yet some unbioturbated deposits may have been deposited under anoxic conditions. Hydrodynamic energy controlled facies distribution: facies M_{cr}b was formed during times of low-velocity currents and less mobile substrates, whereas the other facies record times of higher-energy currents.

4.2. *Facies association 2 (FA2): mixed to calcareous mudstone*

4.2.1. *Description*

This facies association consists of 0.2–5 cm-thick, mixed to calcareous fine mudstone with parallel to low-angle coarse mudstone laminae

Table 1
Summary of contourite drift facies associations (FA).

Facies association	Description	BI	Trace fossils	Interpretation
FA1 Crinoidal, mixed to calcareous mudstone	Dominant: massive, parallel-, low-angle, and ripple cross-laminated crinoidal, mixed to calcareous mudstone (M_{cr}b M_{cr}h, M_{cr}l, M_{cr}r). Subordinate: Planar cross-bedded, and wavy-laminated, crinoidal, mixed to calcareous mudstone (M_{cr}p, M_{cr}w), normal-graded to massive, calcareous fine to coarse mudstone (M_sg, M_sm), and tuff to lapilli ash-tuff (Tg, Tm).	0-1, to 3-6	*Crininicaminus* isp. And *Planolites* isp., *Teichichnus rectus, Phycosiphon incertum*, ? *Skolithos* isp., *Coprulus oblongus* and *Thalassinoides* isp.	Crinoid-rich contourite drift: Reworking by semi-permanent contour currents of low sediment concentration upon a crinoid-rich sediment. Anoxic to upper dysoxic conditions.
FA2 Mixed to calcareous mudstone	Dominant: Mixed to calcareous fine mudstone with coarse mudstone laminae (Mh, Ml), parallel- to low-angle and current-ripple cross-laminated mixed to calcareous coarse mudstone (M_sh, M_sl, M_sr), and massive, mixed to calcareous fine to coarse mudstone (M_{cm}b). Subordinate: Wave ripple cross-laminated, mixed to calcareous coarse mudstone (M_sw), low-angle cross-bedded peloidal, calcareous mudstone (M_pl) and normal-graded to massive, calcareous fine to coarse mudstone (M_sg, M_sm).	0-2, locally 4-5	*Nereites* isp., *Phycosiphon incertum, Planolites* isp., *Palaeophycus* isp., *Palaeophycus heberti*, escape trace fossils, ?*Lockeia* isp., *Teichichnus rectus, Alcyonidiopsis longobardiae, Coprulus oblongus* and pyrite-rich burrows.	Bioclastic- and silt-rich contourite drift: Traction current transport by semi-permanent contour currents in a bioclastic- and silt-rich seafloor. Anoxic to upper dysoxic conditions.
FA3 Calcareous to mixed mudstone interbedded with calcareous mudstone	Dominant: Calcareous to mixed fine mudstone with coarse mudstone laminae (Mh, Ml), parallel to low-angle, and current-ripple cross-laminated, calcareous to mixed coarse mudstone (M_sh, M_sl, M_sr), and massive, calcareous mudstone (M_cm). Subordinate: Normal-graded, calcareous fine to coarse mudstone (M_sg), composite beds of mixed fine to coarse mudstone (Mcomp) and bindstone (B_m).	0-3, rarely 4	Equilibrium trace fossils, ?*Lockeia* isp., *Lockeia siliquaria*, escape trace fossils and ? *Skolithos* isp.	Mixed drift and fluid-mud deposits: Combination of semi-permanent contour currents and fluid mud deposition, under dysoxic conditions.

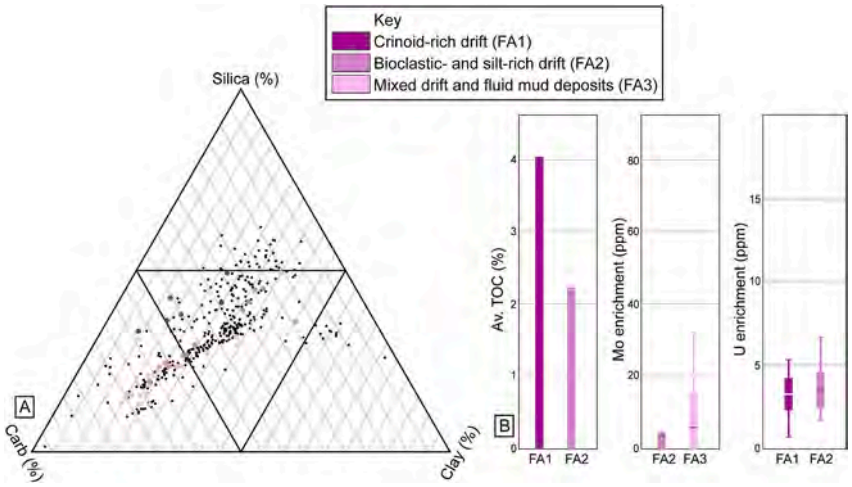

Fig. 6. Geochemical data of the contourite drift facies associations. A) Compositional data from XRD. Black dots represent basin and slope deposits of the Vaca Muerta Formation. B) Average TOC content from cutting samples, Mo enrichment data provided by XRF, and U enrichment from spectral gamma ray data. Median value indicated by a middle line in the box and whisker plots.

(Mh, Ml, Fig. 10), parallel-, low-angle and current-ripple cross-laminated mixed to calcareous coarse mudstone (M_sh, M_sl, M_sr), and 1-30 cm-thick, massive, mixed to calcareous mudstone (M_{cm}b, Fig. 11). Thin-bedded, wave ripple cross-laminated mixed to calcareous coarse mudstone (M_sw), medium-bedded, low-angle cross-bedded peloidal, calcareous mudstone (M_pl), and very thin-to thin-bedded, sharp-to erosive-based, normal-graded to massive, calcareous fine to coarse mudstone (M_sg, M_sm) are minor constituents. The bases are sharp to erosive with wavy surfaces, or locally gradational. Beds are mostly tabular but occasionally lenticular, representing starved ripples. Laminae are 0.2–3.0 mm thick, showing black-colored, sand-sized, tabular to rounded mudstone intraclasts. The laminae in facies Mh and Ml occur as tabular or lenticular, with a massive to rarely thinly laminated texture (Fig. 10B). Ml laminae can grade laterally to Mh (Fig. 10D). These facies show several reactivation surfaces in a cm-scale, revealed by multiple erosive or sharp bases (Fig. 11A). Ripple cross-lamination shows one predominant orientation in the core (80.5%, n = 180), with minor ripples displaying an apparent opposite direction (19.5%). Erosive structures, such as scour marks, gutter casts, and intraclastic and bioclastic lags, also occur. Minor soft-sediment

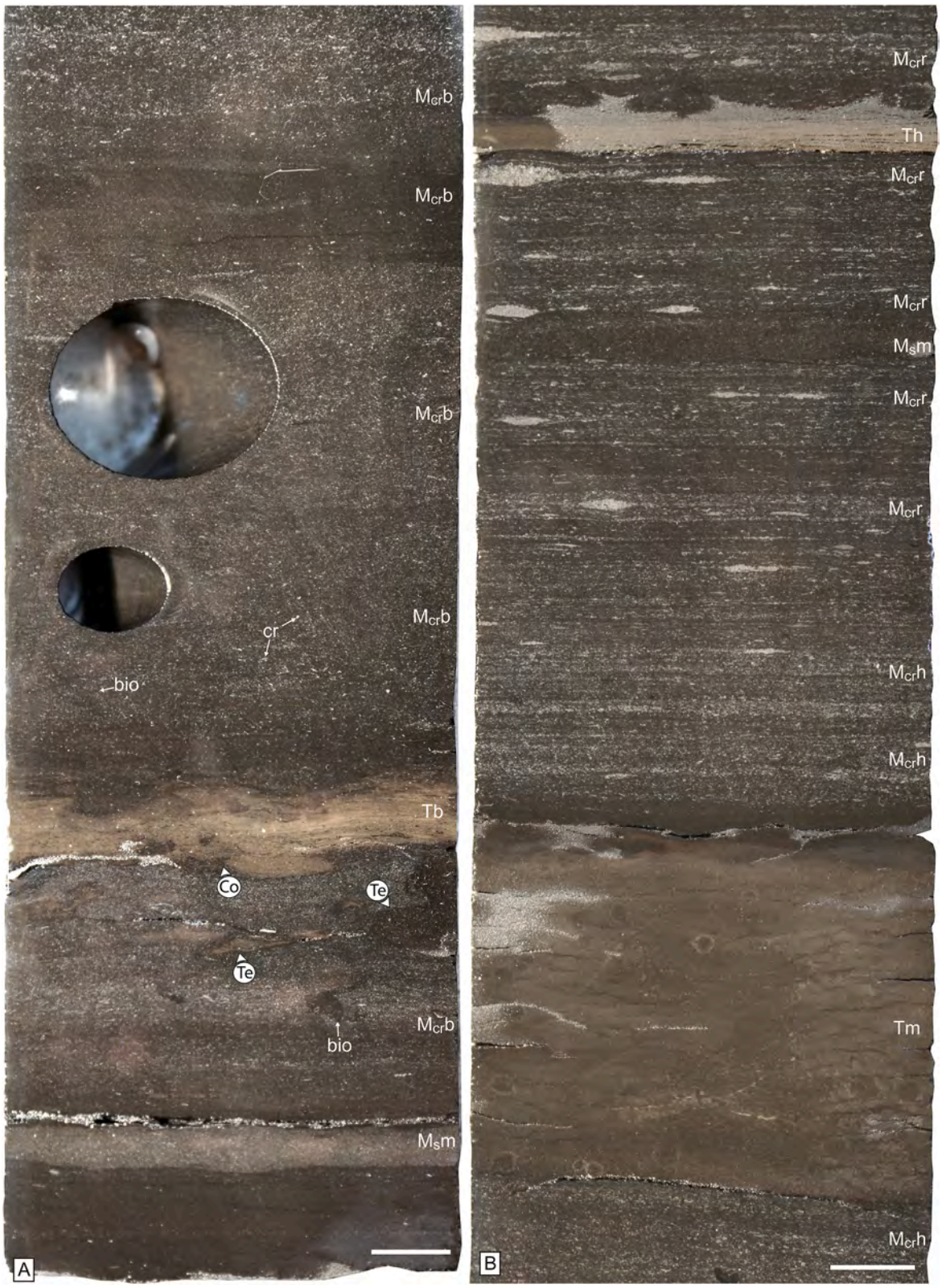

Fig. 7. Crinoidal mudstone of FA1. Scale bars are 1 cm. A) Bioturbated, massive crinoidal mudstone ($M_{cr}b$), interbedded with massive coarse mudstone ($M_s m$) and bioturbated tuffs (Tb), with biodeformational structures (bio) and crinoids (cr) delineated in the image. *Coprulus oblungus* (Co) and *Teichichnus* isp. (Te) Occur in the tuff and mudstone. B) Parallel-laminated crinoidal mudstone ($M_{cr}h$) and mudstone with lenticular structures interpreted as crinoidal ripples ($M_{cr}r$), interbedded with unbioturbated, massive and parallel-laminated tuffs (Tm, Th) and massive coarse mudstone ($M_s m$).

Fig. 8. Crinoidal mudstone of FA1. Scale bars are 1 cm. A, B, C). Crinoid-rich lenticular structures representing bioclastic ripples (br) and constituting ripple cross-laminated mudstone ($M_{cr}r$). Note the ripple foresets in B and C (upside down white arrows). D) Planar cross-bedded crinoidal mudstone ($M_{cr}p$) with erosive bases (eb).

deformation structures include small-sized load casts at the base of beds, syneresis cracks, pseudonodules, and normal synsedimentary microfaults. Average TOC is 2.25% (N = 3).

Petrographic analysis indicates a mixed to calcareous, and rarely siliceous, coarse to fine mudstone with minor very fine-grained sand-sized bioclasts and intraclasts (Fig. 9B). The grains are silt-sized plagioclase, calcite-replaced radiolarians, foraminifera, bivalves, carbonate intraclasts, undifferentiated skeletal fragments, mudstone intraclasts, and minor quartz, pellets and echinoderm fragments, occurring in a matrix with illite and coccoliths. The laminae consist of silt-to very fine sand-sized, demosponge *Rhaxella* fragments, foraminifera, calcite-replaced radiolarians, and mudstone intraclasts (Fig. 9B).

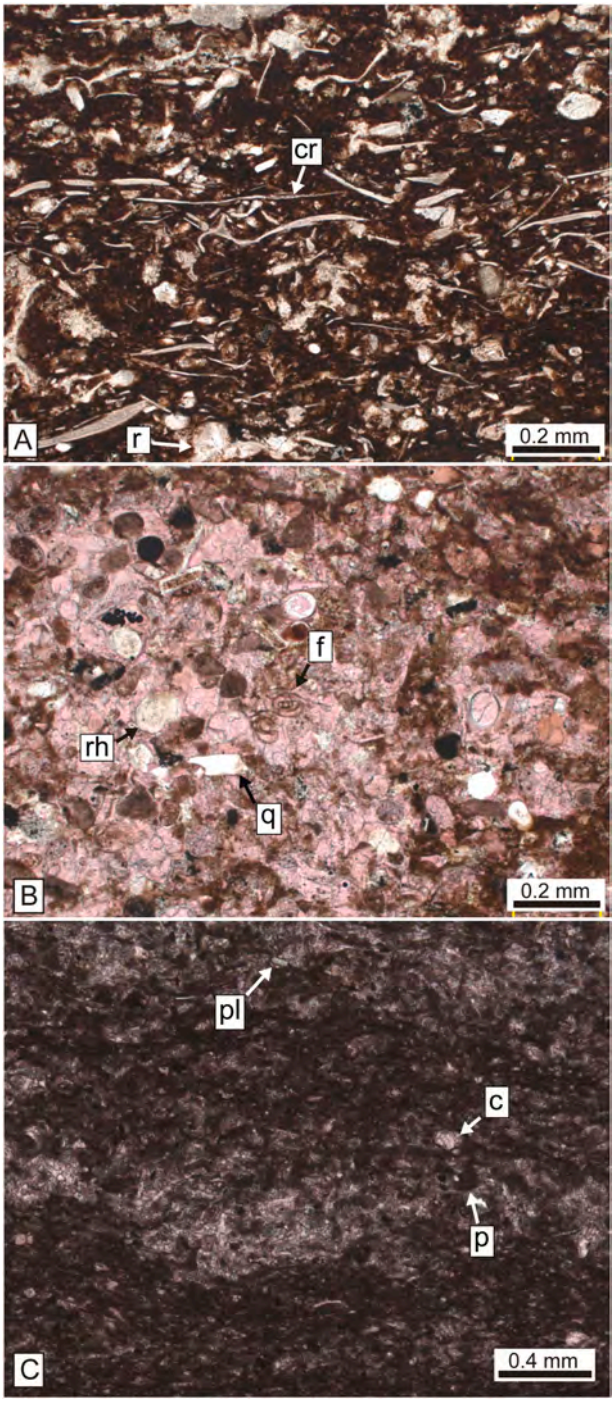

Fig. 9. Thin sections of the deposits interpreted as produced by contour currents of the Vaca Muerta Formation. A) Crinoidal mudstone of FA1, with crinoid ossicles (cr) and minor radiolarians (r). B) Detail of the laminae of the laminated fine to coarse mudstone (M_sh) in FA2, displaying *Rhaxella* sponge fragments (rh), quartz (q) and forams (f). C) Fine to coarse mudstone of FA3 with a lamina cemented by carbonate (lighter interval), showing peloids (p) and carbonate intraclasts (c). Siliciclastics such as plagioclase (pl) occur in the dark mudstone.

The geochemical dataset shows lower Mo and U values compared with deposits from the basin (Fig. 6B).

Degree of bioturbation varies from absent to intense, reaching a BI of 4–5 in facies $M_{cm}b$ (Fig. 11C). Common trace fossils are *Nereites* isp., *Phycosiphon incertum, Planolites* isp., *Palaeophycus* isp., *Palaeophycus heberti,* and escape trace fossils, whereas ?*Lockeia* isp., *Teichichnus rectus, Alcyonidiopsis longobardiae, Coprulus oblongus,* and pyrite-rich burrows are minor constituents. Locally, this facies association is arranged in four discrete 1.7–2.2 m-thick successions showing, bottom up, a decreasing and then an increasing BI. These bigradational successions can be subdivided into two types: type A comprises facies Mh and Ml and a high percentage of $M_{cm}b$ over total thickness (~50–60%), type B shows facies Mh, Ml, M_sh, M_sl and M_sr, a low percentage of $M_{cm}b$ (~15–30%), local presence of M_sw, and intraclastic and bioclastic lags (Figs. 12 and 13).

4.2.2. Interpretation

This facies association represents enhanced contour current activity generating fine-grained sediment drifts. Following terminology from the literature (e.g. Stow and Bowen, 1980; Stow and Shanmugam, 1980), Mh is comparable to the silt laminae encased in fine mud, the minor discontinuous laminae grouped in facies Mh can be correlated with the "wispy lamination", Ml is similar to the "low-amplitude ripples", and M_sr represents current ripples. All the traction structures were generated during bedload sediment segregation from mixed clay-silt suspensions and consequent floccules and silt ripple formation, similarly as in flume experiments (Schieber, 2011; Yawar and Schieber, 2017). Periodic introduction of different sediment grain sizes into the current produced the mixed suspensions that were subsequently sorted during bedload transport (Kuenen, 1966). Facies Mh is laterally associated with current ripples of facies Ml (Fig. 10D) or shows downlap laminae relationships (Fig. 10C), supporting the origin as a low-relief, bedload traction structure compacted during diagenesis (Schieber et al., 2007). In this context, velocities below 25 cm/s were responsible for facies Mh and Ml deposition, whereas over 25 cm/s, facies M_sh, M_sl and M_sr were produced due to transport above the threshold for clay floccule accumulation (Yawar and Schieber, 2017). This hydrodynamic energy change occurs in tandem with increased bed erosion and the amount of sharp to erosive bases. Intraclastic and bioclastic lags reflect periods of increased flow velocity and erosion. This facies association displays multiple recurrence of traction structure deposits alternating with some colonization surfaces, indicative of fluctuating current velocity (Rodríguez-Tovar et al., 2019). The occurrence of facies M_sw suggests oscillatory flow reworking in the coarser-grained deposits (type B successions), associated with long wavelength waves during storms. Alternatively, facies M_sw could be the result of unidirectional, transitional flows rich in clays developing irregular bedforms (Baas et al., 2016).

Facies $M_{cm}b$ is generated due to high bioturbation during low energy current activity. A moderately diverse trace-fossil assemblage, highly bioturbated intervals in comparison with basin deposits, and low values of redox-sensitive trace elements suggest oxygen and food increments associated with the currents (Paz et al., 2022). Moreover, hydrodynamic energy increased from successions type A to type B, characterized by an increase of traction structures and a decrease in the thickness of bioturbated bed ($M_{cm}b$).

Hydrodynamic energy constitutes the prime control for bioturbation in this facies association (i.e. the higher the hydrodynamic energy, the higher the stress over the benthos and the lower the bioturbation intensity; Paz et al., 2022). This is exemplified by the type A and B successions. At the base of the successions, an intermittent current regime and low flow velocities promoted extensive bioturbation and beds were completely homogenized. The middle part records steady currents and higher flow velocities that inhibited bioturbation allowing preservation of sedimentary structures. Locally, colonization surfaces and escape trace fossils indicate current velocity variations (e.g. Rodríguez-Tovar et al., 2019). The top of these successions records a new decrease of energetic conditions allowing organisms to completely rework the sediment. Although grain size trends within the type A and B successions were not observed, these successions are similar to the documented cyclicity of contourite deposits, where an increasing to decreasing grain size pattern is produced by fluctuations in hydrodynamic energy (Gonthier et al., 1984; Stow and Faugères, 2008).

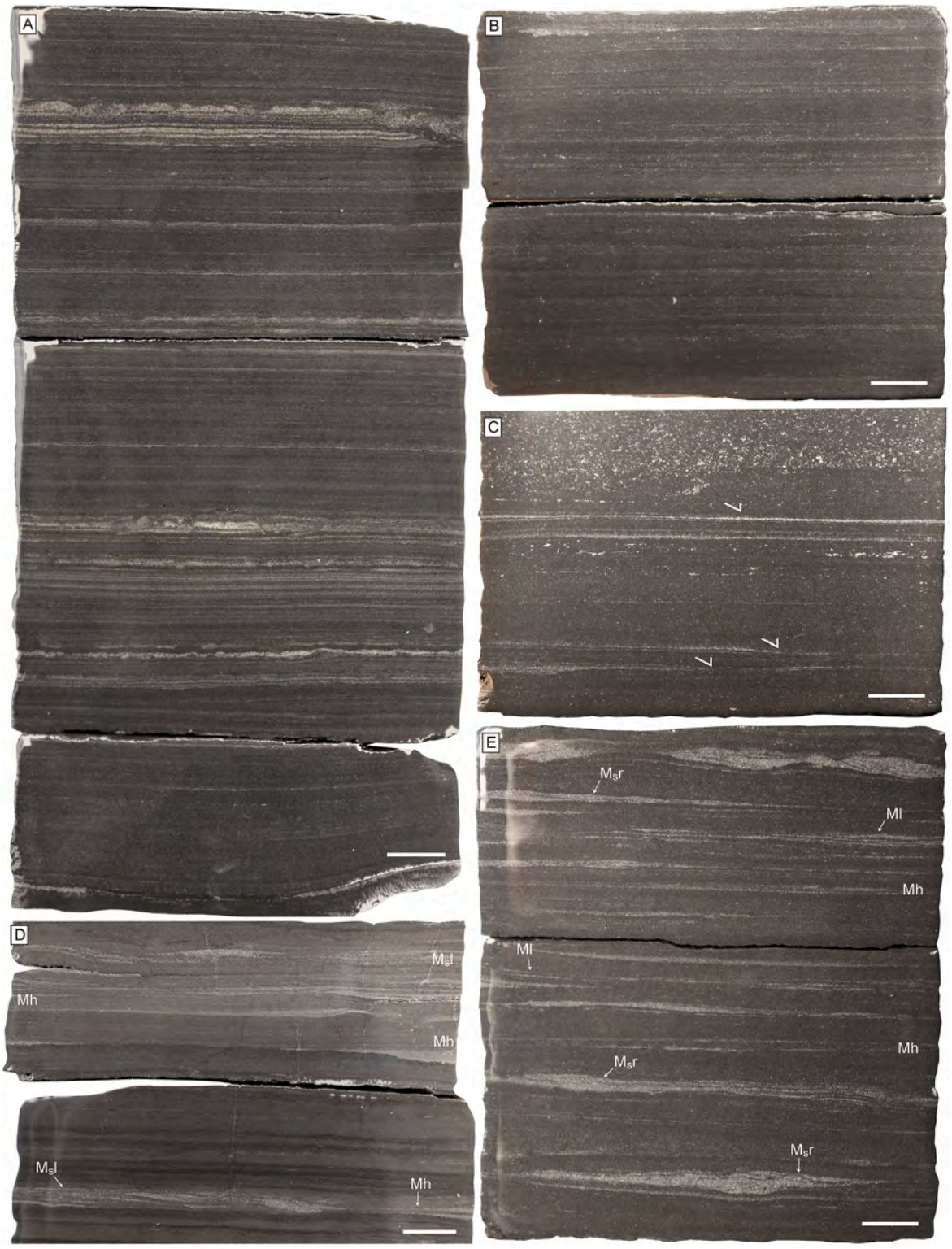

Fig. 10. Core photographs of parallel-to low-angle coarse mudstone laminae encased in fine mudstone (Mh, Ml), and low-angle to ripple cross-laminated coarse mudstone (M_sl, M_sr) of FA2. Scale bars are 1 cm. A) Facies Mh showing small trace fossils. B) Very thin, discontinuous laminae of facies Mh. C) Downlapping relationships in coarse mudstone laminae (Mh). D, E) Facies Mh, Ml, M_sl and M_sr interbedded with fine mudstone. Note the lateral and vertical association of the four facies.

The role of oxygenation on the development of the bigradational BI successions needs to be addressed. In the California Continental Borderland, high oxygenation associated with increased bioturbation during inter-glacial events and high hydrodynamic energy during glacial times were interpreted as factors controlling the preservation/destruction of traction structures (Robinson et al., 2007). In the present case, deposition of the drifts may have been under oxygen-deficient conditions due to the high organic carbon content of the deposits and the dominance of relatively small-sized of burrows (Paz et al., 2022). Therefore, upper dysoxic conditions may have been a background

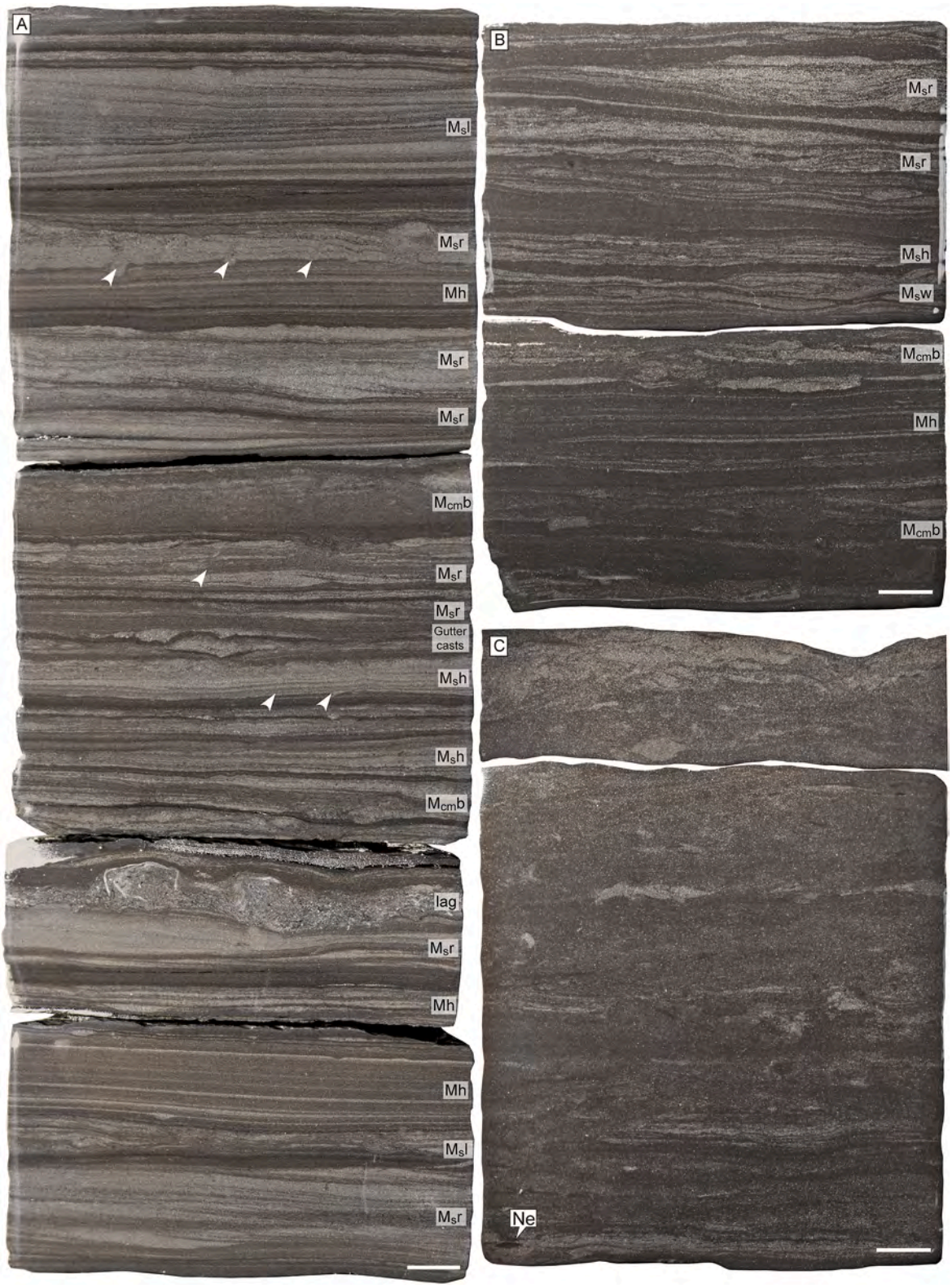

Fig. 11. Core photographs of the coarser-grained facies in FA2. Scale bars are 1 cm. A, B) Parallel coarse mudstone laminae encased in fine mudstone (Mh), parallel-, low-angle and ripple cross-laminated coarse mudstone (M_sh, M_sl, M_sr), and bioturbated mudstone (M_{cm}b), displaying minor small gutter casts and lags. Escape and undetermined trace fossils are indicated with white arrows. C) Highly bioturbated intervals, showing biodeformational structures and *Nereites* isp. (Ne).

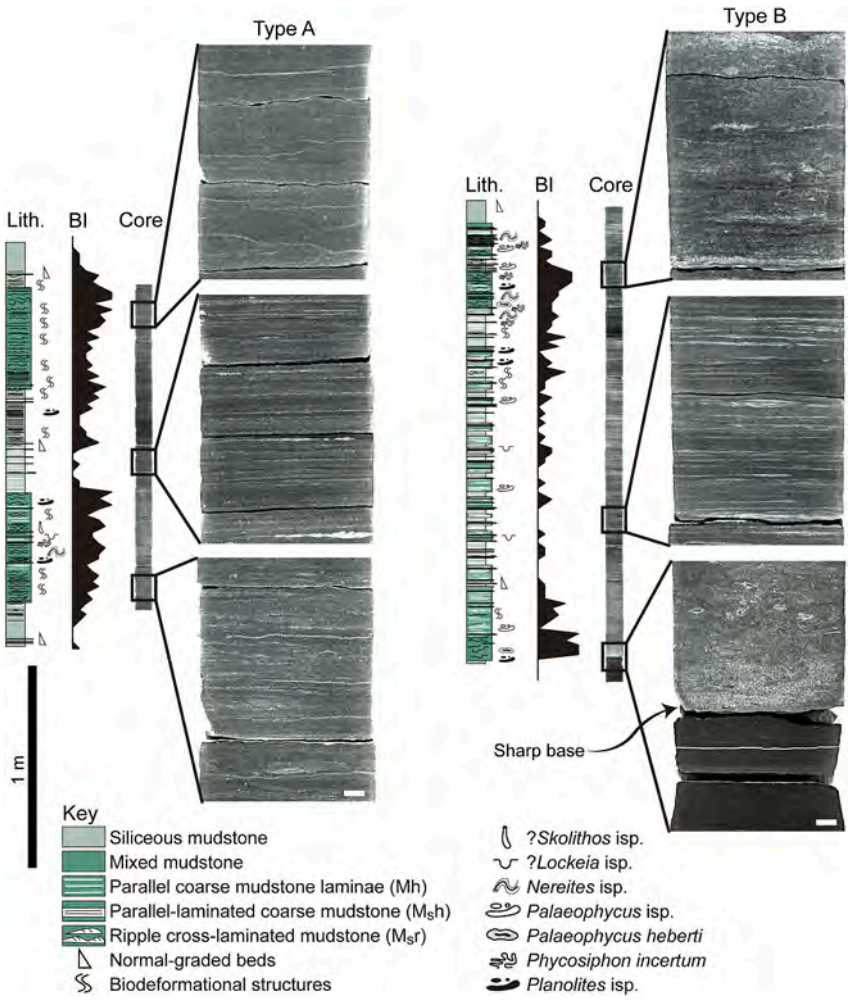

Fig. 12. FA2 characterized by two successions of upward decreasing to increasing bioturbation index (BI), with close-up photographs of the cores (adapted from Paz et al., 2022). Note that the low BI in the middle of both Type A and Type B successions allows preservation of sedimentary structures. Scale bars at the bottom right of the cores are 1 cm.

control during deposition of each succession, overprinted by hydrodynamic energy which, in contrast, fluctuated in intensity. Hence, dysoxia combined with high hydrodynamic energy or local anoxia may explain the preservation of sedimentary structures in the present contourite example.

4.3. Facies association 3 (FA3): calcareous to mixed mudstone interbedded with calcareous mudstone

4.3.1. Description

This facies association is composed by similar facies as in FA2, such as Mh, Ml, M_sh, M_sl and M_sr (Fig. 14), but with a higher calcareous composition (Fig. 6A). In addition, 1-3 cm-thick, sharp-based, massive calcareous mudstone (M_cm) are dominant in this facies association. Normal-graded, calcareous fine to coarse mudstone (M_sg), composite beds of mixed fine to coarse mudstone (Mcomp), and dark, crinkly-laminated, bindstone (B_m) are subordinate. Sharp to erosive bases are common in all these lithologies. The composite mudstone is represented by erosively based, thin-bedded, intraclastic coarse mudstone, followed by parallel-laminated coarse mudstone (Fig. 14A). The massive, normal-graded, and composite mudstone (M_cm, M_sg, Mcomp) shows a mud matrix composed of clays and carbonate mud, and contains tabular, dark bindstone intraclasts, pebble-size, carbonate and mudstone intraclasts, fine-grained sand-sized skeletal and intraclast grains, and silt-sized, quartz, plagioclase, and Fe-dolomite grains (Fig. 9C). Fossils include bivalves and calcite-replaced radiolarians. Local convolute bedding and centimeter-scale synsedimentary normal faults occur.

Variable bioturbation index is observed (BI 0–3 and rarely 4). The trace-fossil content is represented by equilibrium trace fossils, ?*Lockeia* isp., and *Lockeia siliquaria* with minor escape trace fossils and ?*Skolithos* isp. (Fig. 14B, C, D).

4.3.2. Interpretation

This facies association is interpreted as deposited by a combination of low to moderate energy contour currents (similar to Mh, Ml, M_sh, M_sl, M_sr) and fluid mud flows (M_cm, Mcomp) and turbidity flows (M_sg), generating a sediment drift (see also Notta et al., 2017; Reijenstein et al., 2020). The massive and composite mudstone (M_cm, Mcomp) reflects deposition from concentrated density flows to debris flows, whereas the normal-graded mudstone (M_sg) was deposited by mud-rich waning turbidity currents (e.g. Otharán et al., 2020). Bindstone intraclasts in the composite mudstone are restricted to the areas with bindstone, representing a distinct sedimentary structure attributed to erosion and redeposition of bindstone fragments as intraclasts by density flows. Microbial communities generating the bindstone thrived because of larger sand-sized clasts in this facies association, which constitute a favorable substrate for their growth (Noffke, 2010). Equilibrium structures suggest suspension feeding organisms (Mángano et al., 1998), supporting the existence of contour current activity.

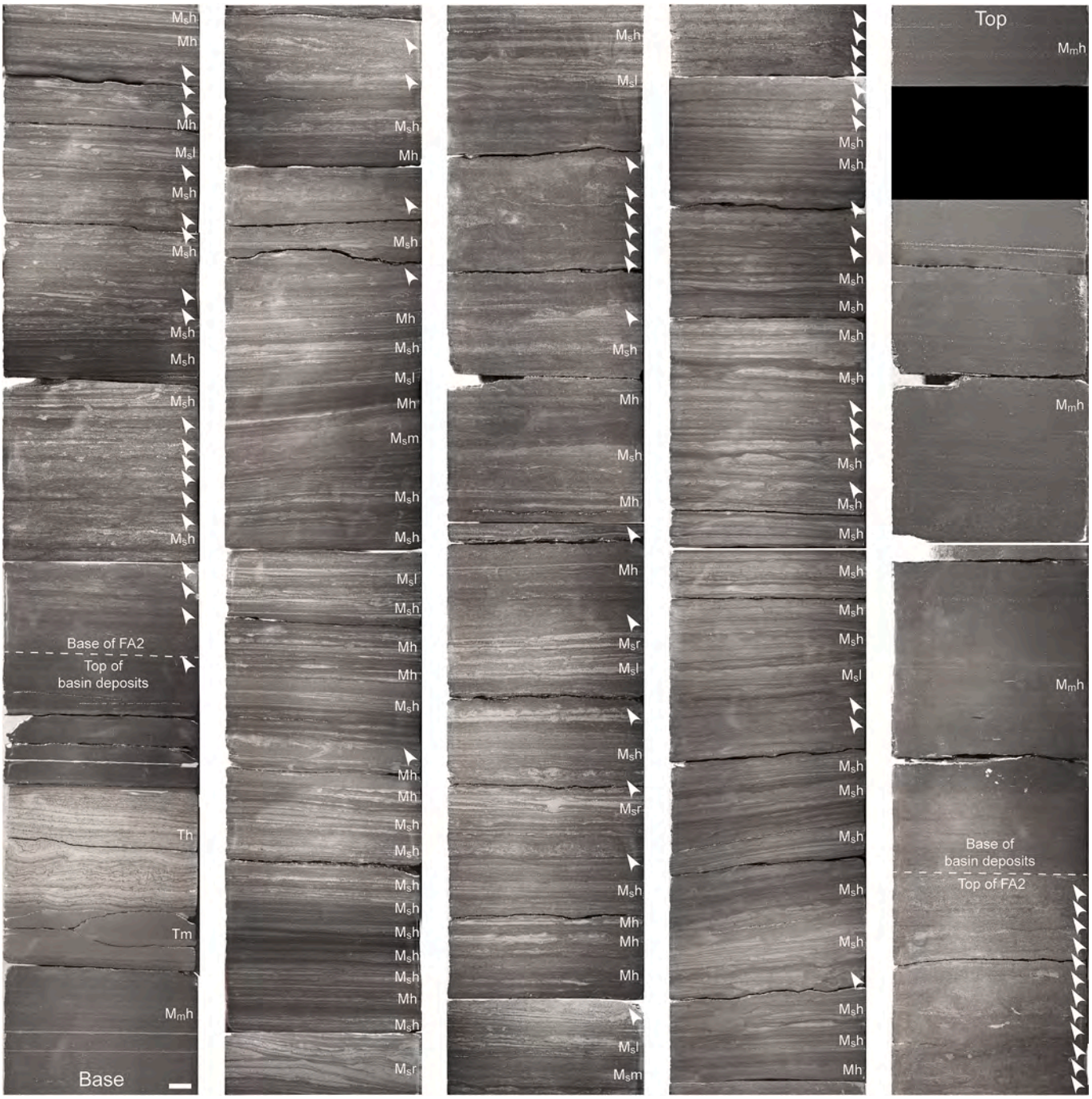

Fig. 13. Type B succession of FA2. Dominant facies are parallel-laminated coarse to fine mudstone (M_sh, Mh), whereas subordinate facies include low-angle and current-ripple cross-laminated, and massive, coarse mudstone (M_sl, M_sr, M_sm). Highly to moderately bioturbated beds are marked with white arrows. Note the abundance of these bioturbated beds towards the base and the top of FA2, reflecting the upward decreasing to increasing bioturbation index. Below and above FA2 are basin deposits, consisting of parallel-laminated, mixed mudstone (M_mh), and massive and parallel-laminated tuff (Tm, Th). Scale bar in the bottom left is 1 cm.

5. Paleoenvironmental and stratigraphic distribution of contourite drift facies association

The Vaca Muerta Formation carbonate-siliciclastic clinoform system record beach, open bay, basin, drift, and slope environments (Paz, 2021). When these deposits are projected on the seismic sections, they can calibrate the acoustic impedance, allowing to infer sedimentary environments in areas where neither cores, nor logs are available. This integration of sedimentology, stratigraphy, and seismic attributes represents a powerful tool to predict rock characteristics. In our case, this correlation highlights that the landward decrease of organic matter and increase of carbonate content is associated with an increase in acoustic impedance from basin to drift to slope environments (Fig. 15A, B, C; Reijenstein et al., 2020).

The stratigraphic distribution of contour current deposits can be framed within the sequence stratigraphic study of wells 1 and 2 (Paz, 2021), as proposed by other authors that analyzed the study area (Fig. 15; e.g., Repol et al., 2014; Notta et al., 2017, 2020; Desjardins and Aguirre, 2018; Minisini et al., 2020b). Considering basin infill as a first-order sequence, the succession shows three third-order sequences developed during deposition of Units 1 and 2 (Desjardins et al., 2018; Minisini et al., 2020a, Fig. 15D). Depositional Sequence 1 (DS1) consists

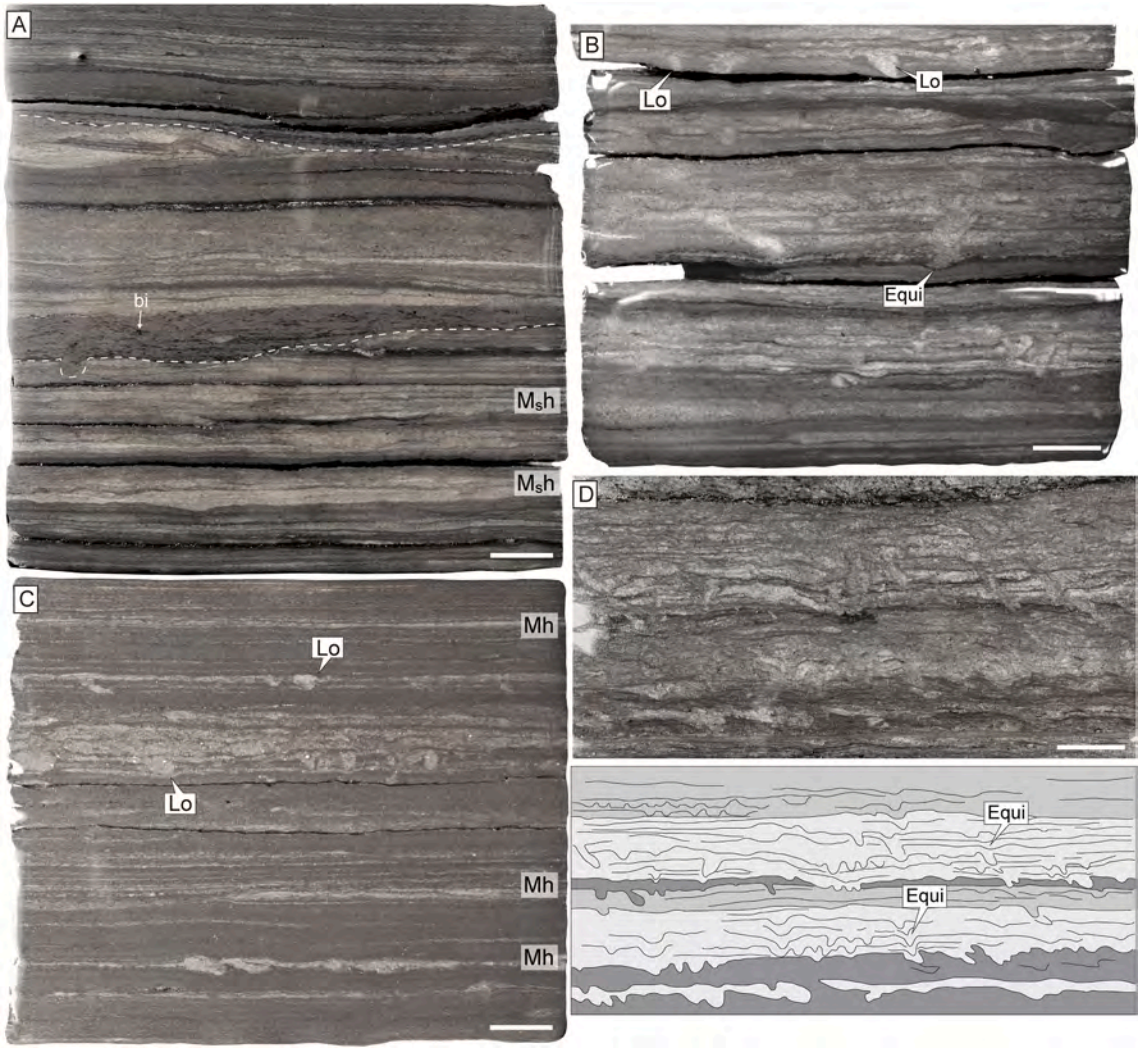

Fig. 14. Photographs of FA3 showing mixed contour current (M_sh, Mh) and fluid mud flow (composite mudstone) sedimentation. Scale bars are 1 cm. A) Composite mudstone beds (bed bases delineated with a dashed line) comprising a basal, intraclastic mudstone, parallel-laminated coarse mudstone and normal-graded mudstone, containing bindstone intraclasts (bi). Contour current facies, such as parallel-laminated coarse mudstone (M_sh), are intercalated. B) ?*Lockeia* isp. (Lo), locally displaying equilibrium structures (Equi). C) Coarse mudstone laminae encased in fine mudstone (Mh), with ?*Lockeia* isp. (Lo). D) Photograph and drawing of intervals with dense occurrence of equilibrium structures (Equi).

of a Transgressive Systems Tract (TST) deepening towards starved basin conditions and a Highstand Systems Tract (HST) within anoxic basin deposits. A sharp sea-level fall prompted the accumulation of oxic basin deposits and crinoid-rich drift facies association (FA1) above anoxic basin deposits, defining a Falling Stage Systems Tract (FSST). On top, the succession shows an aggradational pattern with a repetition of FA1, delineating the Lowstand Systems Tract (LST) of Depositional Sequence 2 (DS2). Four 0.5–4 m-thick, crinoid-rich drift deposits (FA1) are interbedded in both the FSST and LST. The lower three drift deposits show a decrease in thickness in a seaward location, whereas the upper drift deposit only occurs in well 1 (Fig. 4). DS2 continues with a TST characterized by the development of dysoxic basin deposits on top of oxic basin facies deposits, displaying one 1.5 m-thick, bioclastic- and silt-rich drift (FA2), only observed in well 1. On top, a HST comprises progradational stacking patterns associated with resuming regressive conditions of the clinoform system. Five 0.2–2 m-thick, bioclastic- and silt-rich drifts (FA2) occur in well 1. The lower two drift deposits are only recorded in well 1, whereas the upper three drift deposits can be correlated to well 2 (Fig. 4). Above, a FSST triggered extensive contour current activity (FA3 of Well 2, 13 m-thick), and a sharp seaward change of facies associated with slope and fluid mud-rich slope deposits on top of oxic basin deposits (Paz, 2021). The sharp facies change generated truncation of the seismic reflections below, due to sediment erosion and transport associated with the establishment of the contourite system (Fig. 15D). This FSST has been mapped in seismic data as a 5 km-wide, 20 km-long and 25 m-thick, along-slope geobody interpreted as a contourite drift (Reijenstein et al., 2020). Depositional sequence 3 (DS3) comprises a LST consisting of aggradation of fluid mud-rich deposits, whereas above, shutdown of fluid mud activity resulted from deepening conditions of a TST.

6. Discussion

6.1. Presence of bottom currents in the Vaca Muerta Formation

Differentiation between the depositional products of bottom currents and sediment-gravity flows has been a matter of debate for a long time because of the interplay of these two oceanographic processes in deep-marine environments and many shared characteristics (Heezen and Hollister, 1964; Heezen et al., 1966; Hollister and Heezen, 1972; Stow and Lovell, 1979; Shanmugam et al., 1993a, 1993b; Stanley, 1993; Stow et al., 1998; Shanmugam, 2006, 2017; Hüneke and Stow, 2008; Mulder

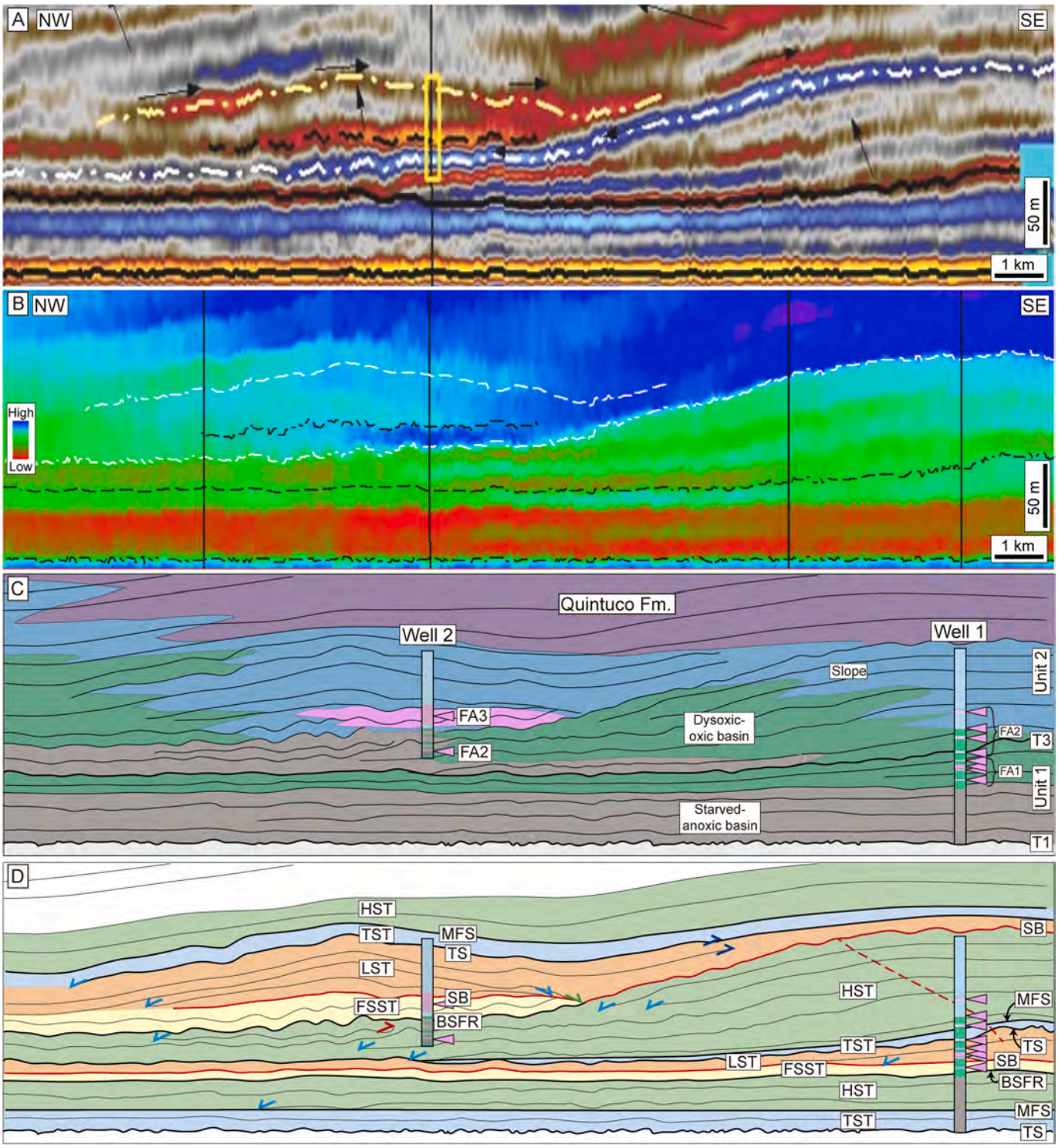

Fig. 15. Stratigraphic analysis of the Vaca Muerta Formation and stratigraphic position of the contourite facies association from seismic data correlating wells 1 and 2. A, B) NW-SE seismic reflections and acoustic impedance cross sections (from Repol et al., 2014 and Notta et al., 2017; see location of wells in Fig. 1). Lower impedance correlates with organic-rich mudstone, whereas higher impedance with carbonate-rich mudstone. C) Environmental interpretation derived from Paz (2021) and impedance from image above. Pink arrows show the location of contourite drift facies associations (FA1, FA2, FA3) in the wells. The thick pink interval in well 2 is the geobody described by Reijenstein et al. (2020), which corresponds to FA3. Starved and anoxic basin deposits (grey) correlate with red colors in the impedance image A, the dysoxic and oxic basin (green) and drift (pink) deposits with green and blue impedance colors, and the slope (light blue) with blue and light blue impedance colors. D) Sequence-stratigraphic interpretation based on stratal termination analysis and facies stacking patterns. Light blue arrows = downlap, blue arrows = toplap, red arrows = truncation, green arrows = offlap, TS = Transgressive Surface, MFS = Maximum Flooding Surface, SB = Sequence Boundary, BSFR = Basal Surface of Forced Regression, TST = Transgressive Systems Tract, HST = Highstand Systems Tract, FSST = Falling Stage Systems Tract, LST = Lowstand Systems Tract. (For interpretation of the references to color in this figure legend, the reader is referred to the Web version of this article).

et al., 2008; Stow and Faugères, 2008; Mulder, 2011; Rebesco et al., 2014; Alonso et al., 2016). Episodic turbidity and hyperpycnal flows are responsible for the most common gravity-flow deposits that may be confused with bottom current deposits. For instance, both low-density turbidity flows (*sensu* Stow and Shanmugam, 1980) and bottom currents (Shanmugam et al., 1993a, 1993b; Shanmugam, 2006) record traction transport at the base of the flow. The associated deposits differ by the vertical arrangement of sedimentary structures: turbidites typically record traction structures from a waning flow, whereas bottom current deposits do not (Martín-Chivelet et al., 2003). Hyperpycnal flow deposits share an additional characteristic with bottom currents: inverse-to-normally graded beds due to waxing-to-waning flows that can be confused with the similar bi-gradational energy profile of contourites (Mulder, 2011).

In this section, the evidence favoring a bottom current interpretation for the facies described in Fig. 16 is summarized (for an alternative interpretation of facies included in FA3, see Kietzmann et al., 2020a). The observed dataset cannot be interpreted as downwelling, storm-induced return flows (producing tempestites) because some of these deposits are too deep (200–400 m; Minisini et al., 2020b) to be considered above storm wave base of an epicontinental sea (<50 m, Schieber, 2016). However, rare storm influence and symmetrical ripples are observed in FA2, indicating a higher contribution of storms towards shallower areas.

6.1.1. *Evidence of semi-permanent currents*

In modern environments, bottom currents of contour-current type affect the seafloor during long periods of time (kyr to Myr; Stow and Faugères, 2008), depending on latitude, seafloor morphology, climate, or eustatic changes. This is in clear contrast with episodic sedimentation resulting in deposition of event beds (e.g. turbidites, tempestites, hyperpycnites). For instance, turbidites have a recurrence of 1 event per 1–150 ky (Talling, 2014 and references therein). However, other processes may have a higher recurrence in the rock record (gravity flows associated with failures of delta fronts or canyon heads, 0.1–5 events per year, Talling, 2014 and references therein; hyperpycnal flows, 1 event per 1–10 years, Johnson et al., 2001; Warrick and Milliman, 2003).

Event beds display a bioturbated top that is developed during flow pauses (e.g., Stow and Shanmugam, 1980; Ponce et al., 2007; Buatois et al., 2011), whereas beds recording bottom current activity show traction structures with an unbioturbated sharp upper contact (Shanmugam et al., 1993a, 1993b; Ito, 2002; Martín-Chivelet et al., 2003; Shanmugam, 2006). Accordingly, the absence of normally graded or bioturbated bed tops suggests a lack of post-event bed, hemipelagic sedimentation. Therefore, sharp upper bed contacts associated with many of the contour current facies in our dataset indicate a continuous current of semi-permanent duration (e.g. Fig. 10D and E, 11, 13).

In addition, the occurrence of low bioturbation intensity in the middle of the type A and type B bi-gradational successions supports the idea of semi-permanent currents generating a continuous hydrodynamic energy stress on the ichnofauna (Figs. 12 and 13). In other words, the intervals rich in traction structures (represented by facies Mh, Ml, M_sh, M_sl, M_sr, M_{cr}h, and M_{cr}r) are interpreted as deposited by semi-permanent currents that precluded the establishment of an infauna associated with background, post-event (fair-weather) deposition, as most burrows can be emplaced within days after deposition (Wheatcroft et al., 1989). A single event explanation for the type A and B bi-gradational successions is rejected due to the existence of a few colonization surfaces (Fig. 11A) and the intercalation of tuffs (Fig. 7A).

From paleontologic and ichnologic datasets, semi-permanent current activity can be inferred from the presence of suspension feeding organisms, which can take advantage of subhorizontal currents delivering

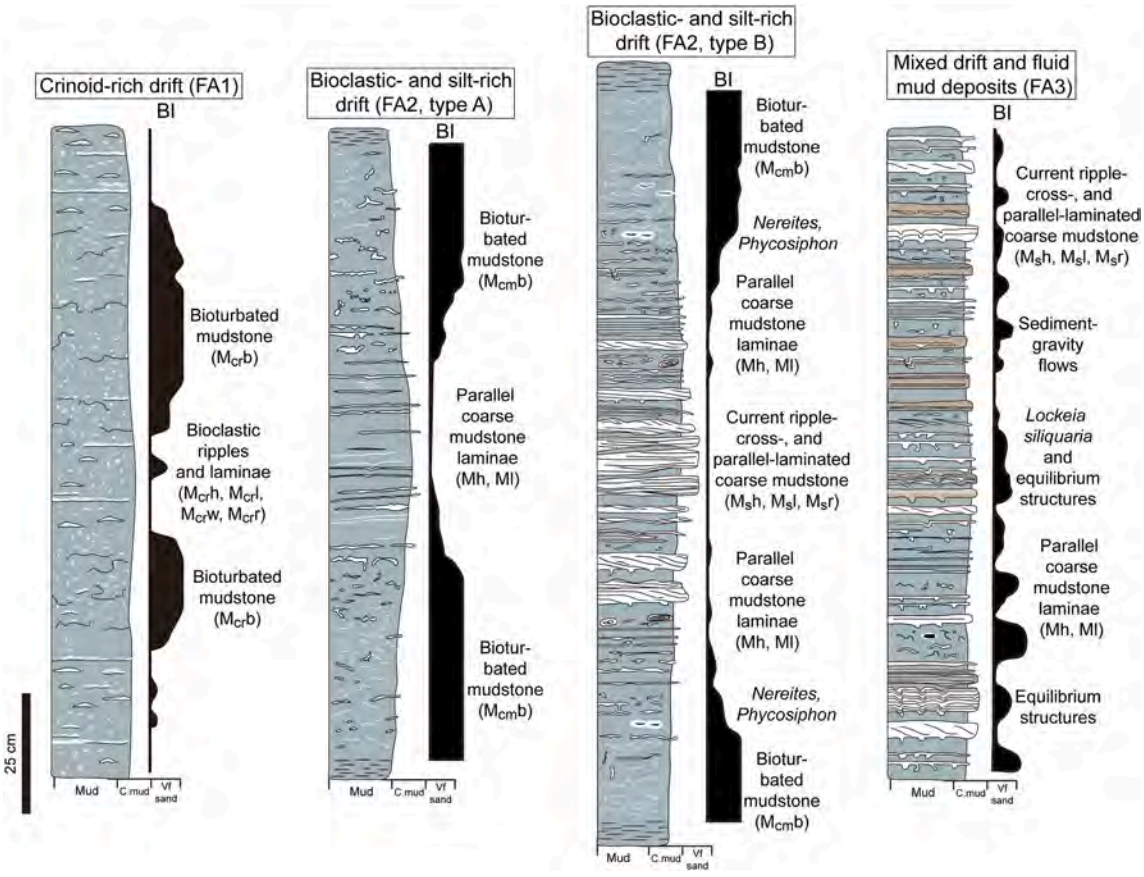

Fig. 16. Idealized facies succession for contour current deposits documented from the Vaca Muerta Formation (adapted from Paz et al., 2022), displaying lithology, sedimentary structures, trace fossil content, and bioturbation index (BI).

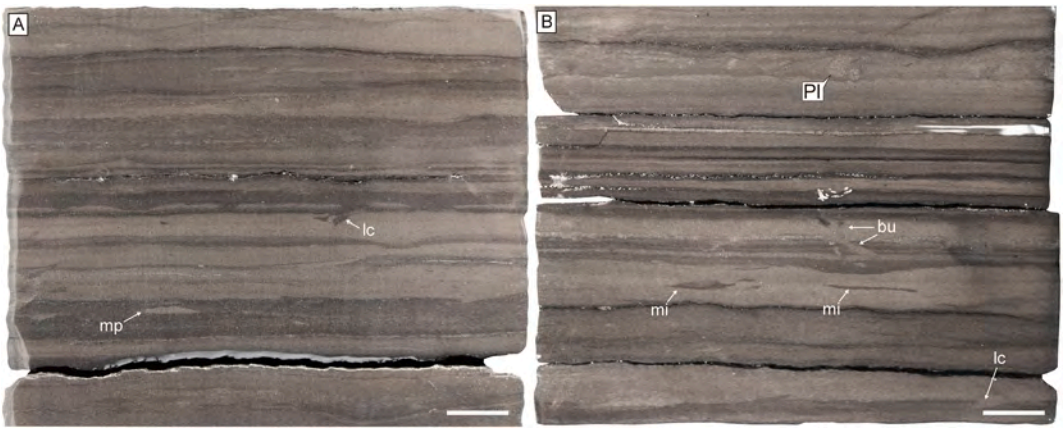

Fig. 17. A, B) Examples of sediment-gravity flows observed in the Vaca Muerta Formation (from Paz, 2021; not analyzed in the present study). Light beds are rich in coarse, calcareous mudstone whereas dark beds consist of fine mudstone. Massive and graded mudstone with minor silt laminae is common, displaying mudstone pseudonodules (mp), load casts (lc), mudstone intraclasts (mi), unidentified burrows (bu) and *Planolites* isp. (Pl). Scale bars are 1 cm.

food (Flach and Thomsen, 1998; Lavaleye et al., 2002). Equilibrium structures in FA3 (Fig. 14B, D) are interpreted as produced by bivalves keeping pace with sedimentation, establishing a connection with the seafloor to feed from suspended food (Mángano et al., 1998; Paz et al., 2022). *Crininicaminus* isp. and *Palaeophycus heberti* (observed in FA1 and FA2) have been interpreted as domiciles of suspension feeders, although they can also be associated with detritus-feeding or predatory organisms (Ettensohn, 1981; Pemberton and Frey, 1982). In addition, although other modes of life have been proposed (e.g. benthic, Milsom, 1994), the *Saccocoma* crinoids were interpreted in other areas as pelagic suspension feeders (Hess and Etter, 2011), indicating the existence of a current system in the water column associated with FA1. This interpretation agrees with the local preferential occurrence of cold-water corals (sessile suspension feeders) on the path of contour currents of the Atlantic Ocean, Gulf of Mexico, and Mediterranean Sea (Hübscher et al., 2010; Hebbeln et al., 2016), although these types of corals have not been reported for the Vaca Muerta Formation.

In summary, sedimentologic characteristics (existence of many sharp upper bed contacts), bioturbation patterns associated with the vertical arrangement of facies (bigradational successions showing unbioturbated middle parts), and ichnologic and paleontologic data (trace and body fossils of suspension feeding organisms, Paz et al., 2022) support the idea of semi-permanent current activity at the seafloor.

6.1.2. *Evidence of low sediment concentration*

Bottom currents represent flows with low sediment concentration. For example, contour currents show concentrations of <0.01–10 mg/L (Hollister, 1993; Tucholke, 2002), cascading events display concentrations of 40 to more than 68 mg/L (Canals et al., 2006; Palanques et al., 2006), and internal tides develop peaks of ~200 mg/L (Puig et al., 2013). Abundant traction structures are encountered in modern examples of deep-marine seafloors affected by bottom currents, due to dominant traction transport at the base of the flow (e.g., Heezen and Hollister, 1964; Heezen et al., 1966). Mud floccule ripples created in flume experiments were produced under suspended sediment concentration of tens of mg/L (Schieber and Southard, 2009). Therefore, bottom-current reworked deposits show rare massive (by *en masse* deposition) or graded beds (Shanmugam et al., 1993a, 1993b; Shanmugam, 2017; Martín-Chivelet et al., 2003; 2008), and common laminated and rippled facies, as found in the described facies associations. Although laminated and rippled facies are also common in turbidites, in our dataset they are not part of the typical Bouma sequence (Tc; Figs. 10 and 11).

In contrast, sediment-gravity flows are characterized by high sediment concentration because excess density is necessary to generate gravitational forcing in the case of a low-angle seafloor, such as the Vaca Muerta foresets and bottomsets in Unit 1 (0.1–0.3° angles, Desjardins et al., 2018; Minisini et al., 2020b). For example, flood waters require high sediment concentrations to plunge and trigger a river-derived, hyperpycnal flows (1 g/L, Parsons et al., 2001), and fluid mud flows and storm surge return flows need to overcome Coriolis forces deflecting transport along-shore (>1 g/L, Myrow and Southard, 1996; >10 g/L, Traykovski et al., 2000). Modern observations of wave- and current-enhanced sediment gravity flows in low-angle slopes, suggest the need of depth-averaged sediment concentrations of 8–150 g/L for flows to be transported offshore, depending on ambient currents (Wright et al., 2001). For instance, concentration values of up to 6 g/L were recorded during wave resuspension events in low angle shelves (*ca* 0.25°), but these suspensions were redistributed by ambient shelf currents, not downslope (Traykovski et al., 2000). Moreover, if compared with sand-rich flows, these high concentration, mud-rich flows present minor turbidity restricted to the base and a dominance of laminar conditions due to the high cohesiveness of the mud (Baas and Best, 2002; Baas et al., 2011). The final deposit may be massive or graded with soft-sediment deformation structures due to the development of upper transitional or quasi-laminar plug flows of high cohesive strength (e.g. Baas et al., 2011).

Sediment-gravity flow deposits in the Vaca Muerta Formation comprise very thin to thin-bedded, massive calcareous medium to coarse mudstone, showing load casts, mudstone pseudonodules, flame structures, and pebble-sized, deformed intraclasts indicating soft-sediment deformation (Fig. 17; Paz, 2021). Muddy hyperpycnites in the SW Neuquén Basin contain deformed mudstone intraclasts (Paz et al., 2019). All these deformation structures suggest high sediment concentration and laminar flow transport in high cohesive strength flows, contrasting with the characteristics of low-concentration bottom currents (Shanmugam, 2006). The fine-grained turbidite model (*sensu* Stow and Shanmugam, 1980) and several muddy hyperpycnite examples (Bhattacharya and MacEachern, 2009; Wilson and Schieber, 2014) show an abundance of soft-sediment deformation structures, such as convolute lamination, load casts and pseudonodules, as well as mantle and swirl structures representative of bioturbation in soupy substrate conditions (Lobza and Schieber, 1999). In addition, sandy hyperpycnites display evidence of soft to soupy substrate conditions, including compacted *Thalassinoides* (Buatois et al., 2011). Sandy hyperpycnites also contain biodeformational structures and *Tasselia* (Olivero and López-Cabrera, 2010; Carmona and Ponce, 2011), a trace fossil associated with soupground conditions (Wetzel and Bromley, 1996). The soft to soupy sediment consistency is related to the liquefied nature of sediment-gravity flows due to water trapping at high sediment concentrations. All these characteristics can be used to infer high sediment concentration in sediment-gravity flows, which clearly contrast with the

sediment loads of bottom currents.

Thus, both the abundance of traction structures and relative low amount of soft-sediment deformation structures in our dataset indicate the existence of a bottom current of low sediment concentration.

6.1.3. Evidence of long-term oxygen supply

In areas with background anoxic to dysoxic conditions, oxygen and food supplied by bottom currents can generate highly bioturbated intervals (Wetzel et al., 2008), whereas sediment-gravity flows cannot sustain long-term oxygenation and would produce the "doomed pioneer" ichnofabric (isolated *Thalassinoides* and *Gyrolithes* encased in unbioturbated laminated dark mudstone; Föllmi and Grimm, 1990). For example, in the Santa Barbara Basin, USA, turbidity currents were able to introduce oxygen in the deeper, oxygen-deficient areas, but the basin chemistry was restored after one month (Sholkovitz and Soutar, 1975). In the Vaca Muerta Formation, wave-influenced, sandy and muddy hyperpycnal lobes, channels and overbanks encased in anoxic, hemipelagic deposits are completely unbioturbated, suggesting sediment-gravity flows were not able to modify oxygen levels at the seafloor (Paz et al., 2019).

Therefore, the association of traction structures with dm-scale, highly bioturbated intervals ($M_{cr}b$, $M_{cm}b$; Figs. 7A and 11C), in some cases sharply overlying parallel-laminated mudstone reflecting anoxic conditions of basin deposits (Figs. 12 and 13), suggests oxygen supply by bottom currents (Paz et al., 2022). This is reflected by a higher BI of drift deposits (1.85, n = 894) when compared with the BI of anoxic basin deposits (0.09, n = 9110) or deposits rich in fluid mud flows (0.95, n = 336). Redox-sensitive elements and average TOC decreasing during bottom current activity also indicates an increase in oxygen (Fig. 6B), however, small burrow diameters suggest upper dysoxic conditions. Unbioturbated and sparsely bioturbated intervals may occur in these deposits (e.g. the middle part of type A and type B successions), either caused by long-term, hydrodynamic stress combined with background dysoxic conditions, or by oxygen-deficient bottom currents.

6.2. Origin of the currents in the Vaca Muerta Formation

The cores described were not oriented when retrieved, hence there is no paleocurrent data to understand the direction of current transport. The existence of shelf-derived sediment in the higher-energy FA2 and FA3 (e.g. *Rhaxella* fragments and carbonate intraclasts) indicates an across-shore flow component shedding material from the shelf (Rodríguez Blanco et al., 2020). Nevertheless, plan-view seismic amplitude extraction of the sedimentary body associated with FA3 shows an along-slope elongation, suggestive of along-shore transport (Reijenstein et al., 2020). Rock magnetic analysis to determine paleocurrents are currently under study and may shed light on the paleocurrent directions in the future (e.g. Kohan Martínez et al., 2018).

During deposition of the contourite drift facies associations of the top of Unit 1 and base of Unit 2 (*A. proximus* to *W. internispinosum* ammonite zones), coeval landward deposits strata in the foresets of the clinoform are represented by the Los Catutos Member of the Vaca Muerta Formation, which are host to highly fossiliferous limestone interbedded with marlstone and mudstone deposited during the Tithonian (upper *A. proximus* to *W. internispinosum* ammonite zones; Leanza and Zeiss, 1994; Rodríguez Blanco et al., 2020). In turn, this member was developed while a pure carbonate interval in the topsets (shelf) occurred (*W. internispinosum* ammonite zone interval of the Picún Leufú Formation), displaying wackestone-packstone intercalated with bivalve-oyster floatstone and cross-bedded oolitic grainstone of tidal origin or deposited at bays (Zeller et al., 2015; Parada, 2019; Rodríguez Blanco et al., 2020). High bioturbation intensity, heterolithic bedding, the ichnotaxon *Palaeophycus heberti*, and bivalve trace fossils in the Los Catutos Member (Kietzmann et al., 2014b; Rodríguez Blanco et al., 2020; M. Paz unpublished data), suggests that this Member may be interpreted as a contourite deposit similar to the facies associations of the present study.

The circulation system generating enhanced bottom current activity during this time interval might have been associated with contour currents, which were influenced by atmospheric circulation (wind stress) and buoyancy forces (thermohaline drivers). NE-trending winds during the Kimmeridgian (Spalletti et al., 2011) probably continued into the Tithonian, due to the existence of monsoonal wind patterns (Scherer et al., 2020). Hence, in the study area, NE-directed winds generated counterclockwise surface circulation that affects water depths associated with the topset to upper foreset of the subaqueous clinoform system (Zeller et al., 2015). At deeper water, intermediate water masses producing clockwise circulation may have reworked lower foreset and bottomset locations. This circulation system may have been similar to, or fed by, low-oxygen paleo-poleward undercurrents such as those observed at Eastern Boundary Upwelling Systems (e.g. Peru-Chile Undercurrent, Fonseca, 1989; or the California Undercurrent, Lynn and Simpson, 1990). The more vigorous circulation of this time interval is provided by increased or higher density cascading of high salinity and low temperature, dense waters from shelf areas (topset), originated during times of cold fronts or storms (Eberli and Betzler, 2019; Minisini et al., 2020b; Rodríguez Blanco et al., 2020). NE winds may have acted as cold dry fronts that lowered the temperature of shelfal waters, for instance, in the Picún Leufú shelf. Cascading of surface watermasses changed the chemistry of deep waters, producing the oxygen increase recorded in the studied dataset (e.g. Meier et al., 2006; Coppola et al., 2017). These currents cascaded deeper than during previous warmer periods due to a higher density. Once reaching intermediate or deep waters, they were deflected to the left by the Coriolis force, feeding the clockwise circulation system. This is similar as the pathway of the North Adriatic Dense Water, cascading downslope in the upper slope of the South Adriatic, then along-slope in localities east of the Bari canyon (Foglini et al., 2016), and finally destabilizing and becoming part of the Adriatic Deep Water (Mantziafou and Lascaratos, 2004). Higher-density intermediate water masses may have changed the outflow pattern of the Neuquén Basin, switching towards a stage of deep outflow associated with anti-estuarine (or probably weakened estuarine), basin-wide circulation. Higher current velocity in wells 1 and 2 may have been augmented by the close location to a strait, evidenced by local subsidence associated with normal faults (during deposition of Unit 1) and the activation of the Loma La Lata high (Fig. 1, during deposition of Unit 2; Domínguez et al., 2020a). Similar successions deposited by contour currents occur in marginal seas such as the Adriatic Sea (Verdicchio and Trincardi, 2008b) or the Western Mediterranean Sea (Lüdmann et al., 2012).

Although processes such as tides are unlikely to be amplified enough to trigger basin-wide, long-term changes in seafloor oxygenation, these processes are not completely excluded as possible drivers for bottom current transport (e.g. Kietzmann et al., 2014b; Zeller et al., 2015; Schieber, 2016). Zeller et al. (2015) considered tides as a driver for basin circulation in the Vaca Muerta Formation, based on the evidence of tidal transport on the shelf (Picún Leufú Formation), such as sigmoidal cross-bedding with mudstone drapes, herringbone cross-bedding and inclined heterolithic stratification (Spalletti et al., 2000; Kietzmann et al., 2014b). Nonetheless, Parada (2019) analyzed the same interval and pointed out the absence of tidal sedimentary structures. In our dataset, the black laminae in FA2 are composed of mudstone intraclasts and do not represent mudstone drapes of tidal origin (e.g. massive mud layers with local flame structures; Sato et al., 2011), indicating traction processes of a bimodal, non-pulsating flow (Fig. 11; Baas et al., 2016; Yawar and Schieber, 2017; Canale et al., 2020). Tidal modelling of epicontinental basins indicates that the existence of islands greatly affects the tidal range values of the basin (Wells et al., 2005), suggesting that the volcanic arc with islands to the west might have attenuated the tidal effects in the Neuquén Sea. However, the tidal effects on the Vaca Muerta Formation might be confined to the topsets (shelf), where tidal wave shoaling or resonance might have taken place.

An additional process that can resuspend sediment and maintain

bedforms are internal waves, which propagate along a pycnocline and rework sediment on sloping surfaces (Cacchione and Drake, 1986). Deposits from internal waves have been reported in the Upper Jurassic Rosso Ammonitico Formation in the Betic Cordillera (Spain), where cross-bedded peloidal grainstone and *Saccocoma* packstone with hummocky cross-stratification (HCS) are interbedded with bioturbated, bioclastic wackestone (Pomar et al., 2019). This alternation is interpreted as shifts from anoxic and high-energy conditions, to dysaerobic and calm, and then to aerobic and calm (Pomar et al., 2019). In our case, no HCS were observed neither in the Yesera del Tromen outcrop, nor in core (although narrow samples in cores may hamper visualization of larger scale bedding surfaces). Moreover, internal waves producing sediment wave fields have an across-slope extension of tens of km that is restricted by the range of pycnocline oscillations, which contrasts with the deposits of our dataset (Puig et al., 2007; Ribó et al., 2016). During the end of Unit 1 deposition, contour currents took place in bottomset to foreset areas, indicating an across-slope distance of *ca* 160 km (extending to the outcrop section). Ultimately, future paleocurrent measurements may help to understand the role of internal waves in sedimentation, as these currents may show across-shore orientation that contrasts with the along-shore orientation of contour currents (Urgeles et al., 2011).

In conclusion, the deposits from our dataset can be interpreted as produced by contour currents intensified during times of enhanced cascading of dense, shelf waters. It must be noted that the discussed evidence only applies to the three described facies associations. Other bottom current deposits have been documented in basin deposits of the Vaca Muerta Formation (Paz, 2021), lacking evidence of semi-permanent duration or long-term oxygen introduction. Therefore, other short-term processes, such as internal solitary waves or deep-water flushing reworking, may also be active during deposition. In addition, hemipelagic deposits (although they do not show clear evidence of current activity) may also be deposited by very low-energy bottom currents affecting the sea-floor.

6.3. Sedimentologic implications for the Vaca Muerta Formation

An integrated sedimentologic model for the contourites of the Vaca Muerta Formation is proposed in this study (Figs. 16 and 18). These deposits have been described in outcrops before, yet their origin has been unknown (e.g. Gasparini et al., 1997; Spalletti et al., 1999; Scasso et al., 2002; Kietzmann et al., 2008, 2014a; Kietzmann and Palma, 2009a). Seismic and backstripping analyses estimate a depositional water depth of 200–400 m for the bottomset (Mitchum and Uliana, 1985; Minisini et al., 2020b). In bottomset and foreset locations, riverine and aeolian input from the south provided siliciclastics that mixed with benthic and pelagic carbonate and volcaniclastic material (Leanza et al., 2011; Minisini et al., 2020b). Cascading water masses, clockwise contour currents, and sediment-gravity flows likely generated sediment transport and reworking. Towards the shelf, wind effects might have been dominant, generating a wind-driven, counterclockwise surface current system that drove clinoform progradation by lateral sediment advection in the slope (Zeller et al., 2015). In these shallow locations, wind and tidal currents might have moved mixed sediment from the southeast (Zeller et al., 2015) and east (Fig. 18; from the Loma Montosa deposits in the shelf; e.g. Iñigo et al., 2018). The low fetch of the basin might have generated a shallow storm wave base which affected the shelf (<50 m water depth for epicontinental seas; Schieber, 2016; see also Kietzmann and Palma, 2009a).

In our scheme, although contourites are found in every systems tract, they are most abundant in the FSST of DS1 and LST and FSST of DS2 (Figs. 15 and 18). This interpretation agrees with regional sequence stratigraphic frameworks based on stratal stacking patterns, seismic acoustic impedance, and stratal terminations (Notta et al., 2017; Domínguez et al., 2020a, 2020b). These intervals of low sea-levels are associated with carbonate-rich deposition. Similarly, data from the Picún Leufú shelf indicates that the highest development of hardgrounds and evidence of subaerial exposure is associated with carbonate-rich deposition (*W. internispinosum* ammonite zone; Zeller et al., 2015;

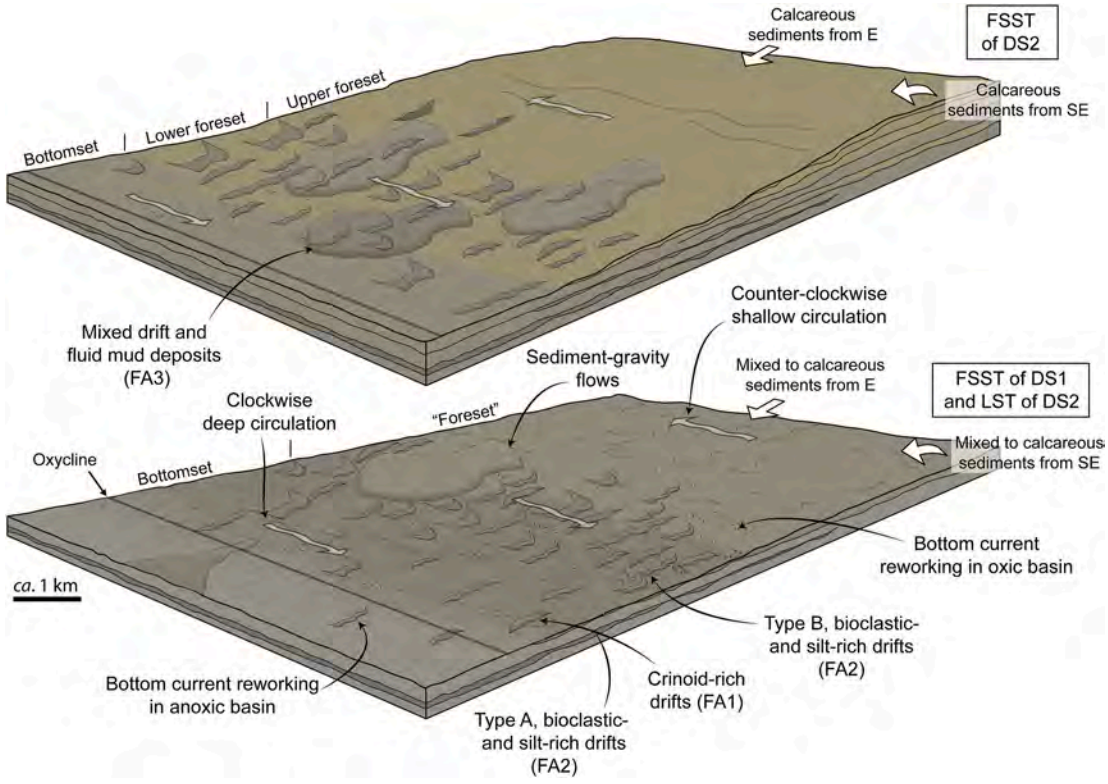

Fig. 18. Block diagram showing the approximate location of contour current deposits in the mixed carbonate-siliciclastic clinoform system of the Vaca Muerta Formation. During FSST of DS1 and LST of DS2, mixed to calcareous deposits occur, whereas calcareous mudstone is dominant in FSST of DS2.

Rodríguez Blanco et al., 2020), correlating with the thickest development of contourites in our dataset (FA3; Fig. 15; top of S-03 of Domínguez et al., 2020a, 2020b). In turn, carbonate-rich intervals are bracketed between the siliciclastic-rich to mixed, early Tithonian (*Virgatosphinctes andesensis* and *Pseudolissoceras zitteli* ammonite zones in Picún Leufú; Paz et al., 2019) and late Tithonian to late Berrasian (*Substeueroceras koeneni* and *Spiticeras damesi* ammonite zones in Sierra de la Vaca Muerta, Zeller, 2013) or early Berrasian (Capelli et al., 2021), suggesting that a decrease of riverine input in the Neuquén Sea generated enhanced carbonate formation. In fact, in the southwest portion of the Neuquén Basin, Krim et al. (2017) analyzed clay minerals and interpreted reduced terrigenous supply for the carbonate interval, associated with either establishment of arid conditions or a decreased size of fluvial catchment areas due to tectonic reconfiguration. However, data from basin centre locations indicate temperate, semi-arid conditions for the whole Tithonian interval (Capelli et al., 2021).

Moreover, times of carbonate deposition might be associated with cooler climates. For instance, during deposition of the Picún Leufú Formation carbonates in the southern part of the basin (late Tithonian–early Berriasian, Leanza et al., 2020), Alberti et al. (2020) recorded a cold snap (18 °C) using bivalve oxygen isotope data. However, Gómez-Dacal et al. (2018) calculated relatively warm temperatures (~25 °C) in the northern Neuquén Basin at the same time. Regional paleoclimatic analysis of southern South America and western Antarctica suggests cool climates and sea-level lowstands during the late Tithonian (Brysch, 2018). An increase in aridity has been documented in Tethyan and Boreal domains for the Tithonian (Hesselbo et al., 2009), in some cases associated with cooler surface waters (Ruffell et al., 2002).

The model that follows is that the contour currents were probably intensified during FSST and LST (Notta et al., 2017; Domínguez et al., 2020b), when low sea-level and decreased fluvial input enhanced bioclastic carbonate production in the topset (Reijenstein et al., 2020), and arid and cooler climates increased the rate and density of cascading events. Zeller et al. (2015) suggested increased carbonate deposition and low current activity during HST due to a lack of accommodation space for current development that decreases siliciclastic input (Zeller et al., 2015). However, the model might be innacurate because HST are times of accommodation space creation (although at a lower rate than sedimentation rate) and accommodation space refers to the space available for sediments (and not for currents) to accumulate (Jervey, 1988). It is likely that the issue resides in using a sequence stratigraphic approach for carbonate deposition (HST carbonates vs. LST siliciclastic) for a subaqueous clinoform system that lacks a siliciclastic-rich LST associated with complete topset subaerial exposure (Reijenstein et al., 2020). Therefore, as inferred from our dataset, HST is associated with siliciclastic- and organic-rich intervals, whereas FSST and LST show carbonate-rich deposition (Fig. 15). Brackenridge et al. (2011) suggested a contourite sequence-stratigraphic model of enhanced current activity during first- or second-order LST associated with enhanced erosion in the shelf. Although the present sequences are of third-order, the Vaca Muerta Formation departs from this model in that arid and cooler climate increased winter convection and were the cause of more vigorous contour current circulation during low sea-levels.

The eight intervals of FA1 and FA2 in Well 1 span a minimum of *ca* 1.21 My (from T2, base of *Aulacosphinctes proximus,* to lower Unit 2, lower *Windhauseniceras internispinosum* ammonite zone; Desjardins and Aguirre, 2018; Kietzmann et al., 2018; Minisini et al., 2020a), hence implying a *ca.* 152 ky minimum recurrence for the intensification of contour currents and indicating a probable control by high-frequency eccentricity cycles (Kietzmann et al., 2015, 2020b). In modern environments, contour currents can be intensified during cooler periods at a kyr scale, due to more vigorous circulation associated with enhanced deep convection (e.g. Baltic Sea, Moros et al., 2020; Mediterranean Sea, Cacho et al., 2000).

In the southern part of the Neuquén Basin, Rodríguez Blanco et al. (2020) have interpreted shelf-sourced carbonates in the Vaca Muerta Formation generated during density cascading. This mechanism is effective in providing oxygen to deeper watermasses (e.g. Meier et al., 2006; Coppola et al., 2017) and explains the complete, basin-wide bottom water oxygenation recorded during contour current activity (Fig. 4). Alternation between basin-wide anoxic and upper dysoxic to oxic conditions was probably controlled by changes in the rate of winter density cascading, which can modify the general circulation pattern of the Neuquén Sea. During times of estuarine circulation, anoxic bottom waters were sluggish and dense, whereas during times of weakened estuarine or anti-estuarine circulation, a higher rate and density of cascading events increased the density and oxygen content of deep waters (Witzke, 1987; Stratford et al., 2000).

The Vaca Muerta Formation occurs at the boundary between mid-latitude arid conditions to the north and warm moist climates to the south (Volkheimer et al., 2008). Therefore, a poleward shift of the arid belt may have triggered arid conditions in the Southern Neuquén Basin, generating a decrease in fluvial input from the North Patagonian Massif (Sagasti, 2005). In turn, the poleward migration of the arid belt might be associated with cooler stages, due to the evidence of lowering water temperatures. The idea of a poleward expansion of the arid belt during cooler climates goes against the fact that the belt is currently migrating poleward under modern global warming. However, Hasegawa et al. (2012) suggested the contrary for the Cretaceous greenhouse climate, with an equatorward shift of the arid belt during warming events when certain CO_2 levels are surpassed (but see Wagner et al., 2013), which may represent an explanation for the increase in aridity in tandem with cooling during the late Tithonian.

The present sedimentologic hypothesis explains the enigmatic occurrence of current activity in relatively deep, basinal locations of the Vaca Muerta Formation, which were previously described as “outer ramp” environments, a depositional setting characterized by infrequent storm reworking (Burchette and Wright, 1992). Backstripping analysis suggest water depths considerably deeper than the location of the storm wave base (200–350 m for the proximal bottomset, Minisini et al., 2020b), and the evidence presented herein precludes the idea of storm-generated flows. Storms were probably the trigger of cascading events originating from the shelf and may have affected the circulation system by increasing its velocity. However, the rate and density of cascading events is mainly controlled by climatic conditions. Relatively shallower areas such as the Mendoza shelf or Picún Leufú record clear HCS structures in peloidal mudstone and sandstone (Kietzmann and Palma, 2011; Paz et al., 2019), indicating a storm wave base associated with basin margin locations.

6.4. Sedimentologic implications for a broader analysis of fine-grained successions

The present study generates different lines of evidence to interpret sedimentary features in fine-grained successions as deposited by contour currents. Where traction structures are abundant and low slope angles preclude sediment-gravity flow transport, the bottom current forcing mechanism represents a plausible process to redistribute mud in distal locations (Schieber, 2016). Moreover, in sediments affected by background oxygen deficiency, the presence of highly bioturbated beds are indeed an evidence of contour current reworking and deep-water oxygen renewal (Stow and Faugères, 2008; Wetzel et al., 2008; Rodríguez-Tovar and Hernández-Molina, 2018; Birgenheier and Moore, 2018). In addition, it must be noted that the evidence of currents with semi-permanent duration, low sediment concentration, and long-term oxygen introduction is not a prerequisite to suggest bottom current activity. Bottom currents can be of short-term duration (e.g. cascading, flushing of deep waters), may support high sediment loads due to sediment entrainment (Shanmugam, 2013), and show low oxygen content (e.g. Sivkov et al., 2002). Minor graded and massive beds with load casts and pseudonodules were also recorded in FA2, implying that high-concentration suspensions can be achieved by these currents.

Interbedded contour current and sediment-gravity flow deposits occur in FA3 (Fig. 14). Reworking of sediment-gravity flow deposits by contour currents constitutes a process documented in modern (Mulder et al., 2008 and references therein) and ancient examples (e.g., Stanley, 1993; Ito, 2002), although debate persists regarding its recognition in the case of ancient deposits (cf., Stanley, 1993; Stow et al., 1998). Sharp upper bed contacts with overlying hemipelagites, better-sorted rippled sands, and a different paleocurrent direction contrasting with the gravity-flow paleocurrent are evidence used in fossil examples to determine contour current activity (Ito, 2002). In our case, current ripples atop and within massive beds indicate contour current reworking, superimposed to gravity flow deposition.

Furthermore, analysis and delineation of these successions have industry applications, as TOC is typically lower in the facies association recording dominant contour current activity (FA1 and FA2; av. TOC of 4.04% and 2.25%, respectively; Fig. 6B) than in basin deposits (av. TOC of 5.06% and 4.77%; Paz, 2021, Fig. 4.18). This fact is related to the enhanced organic carbon remineralization due to bioturbation associated with the oxygenation events of the currents (Aller, 1994; Wetzel et al., 2008) and with a high content of carbonate grains and skeletal components generating TOC dilution. The oxygen content of the along-shore system is influenced by the rate and density of shelf water cascading and the distance from the shelf, because currents decrease their oxygen content as they travel through the organic matter-rich seafloor. Hence, relatively high TOC intervals in FA1 are related with anoxic contour currents in distal positions. The geochemical data also supports the idea of less reducing conditions in the contourite deposits (Fig. 6B). In addition to low TOC, these facies association have low porosity (mainly interparticle) and high water saturation (Facies 3 of Minisini et al., 2020b).

The present fine-grained contourite example has implications with respect to the currently available facies models. Contouritic deposition can be sumarized in two facies models: (1) a model that implies high bioturbation index due to food- and oxygen-rich environments (Faugères et al., 1984; Gonthier et al., 1984; Stow and Lovell, 1979; Stow and Faugères, 2008; Rodríguez-Tovar and Hernandez-Molina, 2018; Dorador et al., 2019), and (2) a model characterized by the abundance of traction structures (Shanmugam et al., 1993a, 1993b; Martín-Chivelet et al., 2003; 2008; Shanmugam, 2006, 2017). This discrepancy was explained due to contrasting energy conditions between low-energy, bioturbated muddy contourites, and high-energy, unbioturbated sandy contourites (Stow and Faugères, 2008; Rebesco et al., 2014). However, the present contribution shows highly bioturbated intervals and successions with relatively well-preserved traction structures in a muddy to bioclastic deposit (Fig. 16), unifying both facies models and demonstrating that sedimentary structures could be preserved in fine-grained depositional environments when stress factors (hydrodynamic energy and oxygen deficiency) limit bioturbation (Paz et al., 2022).

The documented deposits constitute an additional example to the growing list of fine-grained successions where traction structures are considered the product of bottom current reworking (e.g., Pratt, 1984; Schieber, 1994, 1999, 2016; O'Brien, 1996; Loucks and Ruppel, 2007; Singh et al., 2008; Trabucho-Alexandre et al., 2012; Egenhoff and Fishman, 2013; Frébourg et al., 2013; Leonowicz, 2013; Nyhuis et al., 2014; Reisdorf et al., 2014; Birgenheier et al., 2017; Knapp et al., 2017; Ayranci et al., 2018; Li and Schieber, 2018; Minisini et al., 2018). Surprisingly, many of these fine-grained deposits also occur in epicontinental basins affected by oxygen deficiency in their distal settings and showing high organic matter content. The Vaca Muerta Formation differs from other records of bottom current activity mainly by the existence of bioturbation and, in particular, the bigradational bioturbation pattern. In addition, the sharp boundaries at the base and top of some successions with unbioturbated dark mudstone constitute an exceptional preservation of contourites (Figs. 12 and 13), as they delineate the beginning and end of the currents or shifts in the current axis, and facilitated a detailed description of sedimentary processes and environmental controls.

7. Conclusions

In the study area (Neuquén Embayment, Neuquén Basin, Argentina), the Lower Jurassic-Upper Cretaceous Vaca Muerta Formation comprises a mixed carbonate-siliciclastic, subaqueous clinoform system. The sedimentologic analysis focused on crinoidal mixed to calcareous mudstone, mixed to calcareous mudstone, and calcareous to mixed mudstone interbedded with calcareous mudstone, observed in cores from five wells. Twenty-one facies clustered in three facies associations dominated by contour current transport have been defined. The evidence supporting a contour current hypothesis can be summarized as follows: (1) the absence of normal-graded or bioturbated caps, the continuous high hydrodynamic stress observed in the middle of the decreasing to increasing bioturbation index successions, and the suspension feeding organisms, indicate the existence of semi-permanent currents; (2) the high amount of traction structures point towards a flow of low sediment concentration capable of moving sediment across low angle slopes (bottomset and foreset locations); and (3) the existence of highly bioturbated intervals suggests sustained, relatively long-term oxygen introduction to benthic environments by currents. These contour currents were probably directed poleward and reworked bottomset and foreset locations of the clinoform, generating sediment drifts. Due to the correlation with the Los Catutos Member and comparisons with modern analogs, we propose that intensification of the contour current system generating the described dataset was produced by enhanced cascading of cold, dense shelf waters triggered during arid and cool climates. This process represents the most plausible explanation to generate a switch in basin circulation and oxygenate distal areas of the depositional system. The present study supports previous interpretations of sedimentary features such as traction structures and high bioturbation, as produced by contour currents. Differentiation from hyperpycnites, turbidites, and wave- and current-enhanced sediment gravity flows represent a real challenge because bottom/contour currents can be of short-term duration, contain high-sediment concentration, and show low oxygen content. These difficulties suggest that more work is needed in this area to expand our understanding of sediment transport processes in fine-grained sediments.

Declaration of competing interest

The authors declare that they have no known competing financial interests or personal relationships that could have appeared to influence the work reported in this paper.

Acknowledgments

We thank Shell and Tiser S.R.L., and Germán Canto, Adrián Dolso, Sebastián J. Estrada, Sebastián Galeazzi, and Fabián Lamarque from Total Austral S.A. for sharing core information with us. Special thanks to Andreas Wetzel for his valuable comments on an early draft of the manuscript, and to Diego Kietzmann, João Trabucho Alexandre, two anonymous reviewers, and journal editor Ernesto Schwarz for their highly useful feedback. This work was financially supported by the Natural Sciences and Engineering Research Council (NSERC) Discovery Grant [422931-20] to L.A. Buatois, [311727–20] and the George McLeod Enhancement Chair in Geology to M.G. Mángano, PI-UNRN 2017 [40-A-616] and PIP-CONICET [129] to N.B. Carmona, 2016 Student Research Grant from Society for Sedimentary Geology (SEPM), 2016 and 2018 Research Grant from the Geological Society of America (GSA), 2016 Grants-in-Aid Program of the American Association of Petroleum Geologists (AAPG), and 2018 Postgraduate Grant from the International Association of Sedimentologists (IAS).

References

Alberti, M., Parent, H., Garrido, A.C., Andersen, N., Garbe-Schönberg, D., Danise, S., 2020. Stable isotopes ($\delta^{13}C$, $\delta^{18}O$) and element ratios (Mg/Ca, Sr/Ca) of Jurassic belemnites, bivalves and brachiopods from the Neuquén Basin (Argentina): challenges and opportunities for palaeoenvironmental reconstructions. J. Geol. Soc. 178, jgs2020-163.

Aller, R.C., 1994. Bioturbation and remineralization of sedimentary organic matter: effects of redox oscillation. Chem. Geol. 114, 331–345.

Alonso, B., Ercilla, G., Casas, D., Stow, D.A.W., Rodríguez-Tovar, F.J., Dorador, J., Hernández-Molina, F.J., 2016. Contourite vs. gravity-flow deposits of the Pleistocene Faro Drift (Gulf of Cadiz): Sedimentological and mineralogical approaches. Mar. Geol. 377, 77–94.

Ayranci, K., Harris, N.B., Dong, T., 2018. Sedimentological and ichnological characterization of the Middle to Upper Devonian Horn River Group, British Columbia, Canada: insights into mudstone depositional conditions and processes below storm wave base. J. Sediment. Res. 88, 1–23.

Baas, J.H., Best, J.L., 2002. Turbulence modulation in clay-rich sediment-laden flows and some implications for sediment deposition. J. Sediment. Res. 72, 336–340.

Baas, J.H., Best, J.L., Peakall, J., 2011. Depositional processes, bedform development and hybrid bed formation in rapidly decelerated cohesive (mud–sand) sediment flows. Sedimentology 58, 1953–1987.

Baas, J.H., Best, J.L., Peakall, J., 2016. Predicting bedforms and primary current stratification in cohesive mixtures of mud and sand. J. Geol. Soc. 173, 12–45.

Bhattacharya, J.P., MacEachern, J.A., 2009. Hyperpycnal rivers and prodeltaic shelves in the Cretaceous seaway of north America. J. Sediment. Res. 79, 184–209.

Birgenheier, L.P., Horton, B., McCauley, A.D., Johnson, C.L., Kennedy, A., 2017. A depositional model for offshore deposits of the lower Blue Gate Member, Mancos Shale, Uinta basin, Utah, USA. Sedimentology 64, 1402–1438.

Birgenheier, L.P., Moore, S.A., 2018. Carbonate mud deposited below storm wave base. Sediment. Rec. 16, 4–10.

Brackenridge, R., Stow, D.A., Hernández-Molina, F.J., 2011. Contourites within a deep-water sequence stratigraphic framework. Geo Mar. Lett. 31, 343–360.

Brisson, I.E., Fasola, M.E., Villar, H.J., 2020. Organic geochemical patterns of the Vaca Muerta Formation. In: Minisini, D., Fantín, M., Lanusse Noguera, I., Leanza, H. (Eds.), Integrated Geology of Unconventionals: the Case of the Vaca Muerta Play, vol. 121. AAPG Memoir, Argentina, pp. 297–328.

Brysch, S., 2018. Changes in Climate and Palaeoenvironment during the Late Jurassic–Early Cretaceous in Southern South America and Western Antarctica. PhD dissertation. der Ruprecht-Karls-Universität, Heidelberg, p. 233.

Buatois, L.A., Saccavino, L.L., Zavala, C.A., 2011. Ichnologic signatures of hyperpycnal flow deposits in Cretaceous river-dominated deltas, Austral Basin, southern Argentina. In: Slatt, R.M., Zavala, C.A. (Eds.), Sediment Transfer from Shelf to Deep Water—Revisiting the Delivery System, vol. 61. AAPG Studies in Geology, pp. 153–170.

Burchette, T.P., Wright, V.P., 1992. Carbonate ramp depositional systems. Sediment. Geol. 79, 3–57.

Cacchione, D.A., Drake, D.E., 1986. Nepheloid layers and internal waves over continental shelves and slopes. Geo Mar. Lett. 6, 147–152.

Cacho, I., Grimalt, J.O., Sierro, F.J., Shackleton, N., Canals, M., 2000. Evidence for enhanced Mediterranean thermohaline circulation during rapid climatic coolings. Earth Planet Sci. Lett. 183, 417–429.

Canale, N., Ponce, J.J., Carmona, N.B., Parada, M.N., Drittanti, D.I., 2020. Sedimentología e icnología de un delta fluvio-dominado. Form. Lajas (Jurásico Medio), Cuenca Neuquina, Argent.: Andean Geol. 47, 179–206.

Canals, M., Puig, P., Durrieu de Madron, X., Heusnner, S., Palanques, A., Fabres, J., 2006. Flushing submarine canyons. Lett. Nat. 444, 354–357.

Capelli, I.A., Scasso, R.A., Spangenberg, J.E., Kietzmann, D.A., Cravero, F., Duperron, M., Adatte, T., 2021. Mineralogy and geochemistry of deeply-buried marine sediments of the Vaca Muerta-Quintuco system in the Neuquén Basin (Chacay Melehue section), Argentina: Paleoclimatic and paleoenvironmental implications for the global Tithonian-Valanginian reconstructions. J. S. Am. Earth Sci. 107, 103103.

Carbone, O.C., Franzese, J.R., Limeres, M., Delpino, D., Martínez, R., 2011. El Ciclo Precuyano (Triásico Tardío - Jurásico Temprano) en la Cuenca Neuquina. In: Leanza, H.A., Arregui, C.D., Carbone, O.C., Danieli, J.C., Vallés, J. (Eds.), Relatorio del XVIII Congreso Geológico Argentino: Asociación Geológica Argentina, pp. 63–76. Neuquén.

Carmona, N.B., Ponce, J.J., 2011. Ichnology and sedimentology of Miocene hyperpycnites of the Austral Foreland Basin (Tierra del Fuego, Argentina): trace fossil distribution and paleoecological implications. In: Slatt, R.M., Zavala, C.A. (Eds.), Sediment Transfer from Shelf to Deep Water - Revisiting the Delivery System, vol. 61. AAPG Studies in Geology, pp. 171–192.

Casadío, S., Montagna, A.O., 2015. Estratigrafía de la Cuenca Neuquina. In: Ponce, J.J., Montagna, A.O., Carmona, N. (Eds.), Geología de la Cuenca Neuquina y sus Sistemas Petroleros. Fundación YPF, Buenos Aires, pp. 8–21.

Catuneanu, O., 2006. Principles of Sequence Stratigraphy. Elsevier, p. 388.

Cattaneo, A., Correggiari, A., Langone, L., Trincardi, F., 2003. The late-Holocene Gargano subaqueous delta, Adriatic shelf: sediment pathways and supply fluctuations. Mar. Geol. 193, 61–91.

Coppola, L., Prieur, L., Taupier-Letage, I., Estournel, C., Testor, P., Lefevre, D., Belamari, S., Lereste, S., Taillandier, V., 2017. Observation of oxygen ventilation into deep waters through targeted deployment of multiple Argo-O2 floats in the north-western Mediterranean Sea in 2013. J. Geophys. Res. Oceans 122, 6325–6341.

De Castro, S., Hernández-Molina, F.J., De Weger, W., Jiménez-Espejo, F.J., Rodríguez-Tovar, F.J., Mena, A., Llave, E., Sierro, F.J., 2021. Contourite characterization and its discrimination from other deep-water deposits in the Gulf of Cadiz contourite depositional system. Sedimentology 68, 987–1027.

Desjardins, P., Aguirre, H., 2018. Chapter 7: Sierras Blancas. In: González, G., Vallejo, M. D., Kietzmann, D.A., Marchal, D., Desjardins, P.R., González Tomassini, F., Gómez Rivarola, L., Domínguez, R.F., Fantín, M.A. (Eds.), Transecta Regional de la Formación Vaca Muerta–Integración de Sísmica, Registros de Pozos, Coronas y Afloramientos. IAPG, Buenos Aires, pp. 71–82.

Desjardins, P., Fantín, M., González Tomassini, F., Reijenstein, H., Sattler, F., Domínguez, F., Kietzmann, D., Bande, A., Benoit, S., Borgnia, M., Vittore, F., Simo, T., Minisini, D., 2018. Chapter 2: regional seismic stratigraphy. In: González, G., Vallejo, M.D., Kietzmann, D.A., Marchal, D., Desjardins, P.R., González Tomassini, F., Gómez Rivarola, L., Domínguez, R.F., Fantín, M.A. (Eds.), Regional Cross Section of the Vaca Muerta Formation, Integration of Seismic, Well Logs, Cores and Outcrops. IAPG, Buenos Aires, pp. 5–22.

Domínguez, R.F., Leanza, H.A., Fantín, M., Marchal, D., Cristallini, E., 2020a. Basin configuration during the Vaca Muerta times. In: Minisini, D., Fantín, M., Lanusse Noguera, I., Leanza, H.A. (Eds.), Integrated Geology of Unconventionals: the Case of the Vaca Muerta Play, vol. 121. AAPG Memoir, Argentina, pp. 141–162.

Domínguez, R.F., Catuneanu, O., Reijenstein, H.M., Notta, R., Posamentier, H.W., 2020b. Sequence stratigraphy and the three-dimensional distribution of organic-rich units. In: Minisini, D., Fantín, M., Lanusse Noguera, I., Leanza, H.A. (Eds.), Integrated Geology of Unconventionals: the Case of the Vaca Muerta Play, vol. 121. AAPG Memoir, Argentina, pp. 163–200.

Dorador, J., Rodríguez-Tovar, F.J., Mena, A., Francés, G., 2019. Lateral variability of ichnological content in muddy contourites: weak bottom currents affecting organisms' behavior. Nat. Sci. Rep. 9, 17713.

Eberli, G.P., Betzler, C., 2019. Characteristics of modern carbonate contourite drifts. Sedimentology 66, 1163–1191.

Egenhoff, S.O., Fishman, N.S., 2013. Traces in the dark—sedimentary processes and facies gradients in the upper shale member of the upper Devonian–lower Mississippian Bakken formation, Williston basin, north Dakota, USA. J. Sediment. Res. 83, 803–824.

Estrada, S.J., Raverta, M.F., Santa Coloma, M., Torres, J.P., Galeazzi, S., 2020. Pilot phase of the Aguada Pichana Este block, gas window. In: Minisini, D., Fantín, M., Lanusse Noguera, I., Leanza, H.A. (Eds.), Integrated Geology of Unconventionals: the Case of the Vaca Muerta Play, vol. 121. AAPG Memoir, Argentina, pp. 497–514.

Ettensohn, F.R., 1981. *Crininicaminus haneyensis*, a new agglutinated worm tube from the Chesterian of East-Central Kentucky. J. Paleontol. 55, 479–482.

Faugères, J.-C., Gonthier, E., Stow, D.A.V., 1984. Contourite drift molded by deep Mediterranean outflow. Geology 12, 296–300.

Flach, E.C., Thomsen, L., 1998. Do physical and chemical factors structure the community at a continental slope in the NE Atlantic?. In: Baden, S., Pihl, L., Rosenberg, R., Strömberg, J.-O., Svane, I., Tiselius, P. (Eds.), Recruitment, Colonization and Physical-Chemical Forcing in Marine Biological Systems: Developments in Hydrobiology, vol. 132. Springer, pp. 265–285.

Flemming, B.W., 1980. Sand transport and bedform patterns on the continental shelf between Durban and Port Elizabeth (southeast African continental margin). Sediment. Geol. 26, 179–205.

Flemming, B.W., 1981. Factors controlling shelf sediment dispersal along the southeast African continental margin. Mar. Geol. 42, 259–277.

Foglini, F., Campiani, E., Trincardi, F., 2016. The reshaping of the South West Adriatic Margin by cascading of dense shelf waters. Mar. Geol. 375, 64–81.

Föllmi, K.B., Grimm, K.A., 1990. Doomed pioneers: gravity-flow deposition and bioturbation in marine oxygen-deficient environments. Geology 18, 1069–1072.

Fonseca, T.R., 1989. An overview of the poleward undercurrent and upwelling along the Chilean coast. In: Neshyba, S.J., Mooers, ChN.K., Smith, R.L., Barber, R.T. (Eds.), Poleward Flows along Eastern Ocean Boundaries: Coastal and Estuarine Studies, vol. 34, pp. 203–228.

Frébourg, G., Ruppel, S.C., Rowe, H., 2013. Sedimentology of the Haynesville (Upper Kimmeridgian) and Bossier (Tithonian) Formations, in the Western Haynesville Basin, Texas, U.S.A. In: Hammes, U., Gale, J. (Eds.), Geology of the Haynesville Gas Shale in East Texas and West Louisiana, vol. 105. AAPG Memoir, Tulsa, pp. 47–67.

Gasparini, Z., Spalletti, L., De la Fuente, M., 1997. Tithonian marine reptiles of the Western Neuquén Basin, Argentina. Facies and palaeoenvironments. Geobios 30, 701–712.

Gómez-Dacal, A.R., Gómez Peral, L.E., Spalletti, L.A., Sial, A.N., Siccardi, A., Poiré, D.G., 2018. First record of the Valanginian positive carbon isotope anomaly in the Mendoza shelf, Neuquén Basin, Argentina: palaeoclimatic implications. Andean Geol. 45, 111–129.

Gómez Rivarola, L., Borgnia, M., 2018. Chapter 13: San Roque. In: González, G., Vallejo, M.D., Kietzmann, D.A., Marchal, D., Desjardins, P.R., González Tomassini, F., Gómez Rivarola, L., Domínguez, R.F., Fantín, M.A. (Eds.), Transecta Regional de la Formación Vaca Muerta–Integración de Sísmica, Registros de Pozos, Coronas y Afloramientos. IAPG, Buenos Aires, pp. 143–153.

Gonthier, E.G., Faugeres, J.-C., Stow, D.A.V., 1984. Contourite facies of the Faro Drift, Gulf of Cadiz. In: Stow, D.A.V., Piper, D.J.W. (Eds.), Fine-grained Sediments: Deep-Water Processes and Facies, vol. 15. Geological Society of London Special Publications, London, pp. 275–292.

González Tomassini, F., Kietzmann, D.A., Fantín, M.A., Crousse, L.C., Reijenstein, H.M., 2014. Estratigrafía y análisis de facies de la Formación Vaca Muerta en el área de El Trapial, Cuenca Neuquina, Argentina, *in* IX Congreso de Exploración y Desarrollo de Hidrocarburos. Simposio de Recursos No Convencionales: IAPG, Mendoza, pp. 587–611.

Gulisano, C.A., Gutiérrez Pleimling, A.R., Digregorio, R.E., 1984. Análisis estratigráfico del intervalo Tithoniano-Valanginiano (Formaciones Vaca Muerta, Quintuco y

Mulichinco) en el suroeste de la provincia de Neuquén. In: IX Congreso Geológico Argentino, Actas I: Asociación Geológica Argentina, pp. 221–235. Bariloche.
Hasegawa, H., Tada, R., Jiang, X., Suganuma, Y., Imsamut, S., Charusiri, P., Ichinnorov, N., Khand, Y., 2012. Drastic shrinking of the Hadley circulation during the mid-Cretaceous Supergreenhouse. Clim. Past 8, 1323–1337.
Hebbeln, D., Van Rooij, D., Wienberg, C., 2016. Good neighbours shaped by vigorous currents: Cold-water coral mounds and contourites in the North Atlantic. Mar. Geol. 378, 171–185.
Heezen, B.C., Hollister, C., 1964. Deep-sea current evidence from abyssal sediments. Mar. Geol. 1, 141–174.
Heezen, B.C., Hollister, C.D., Ruddiman, W.F., 1966. Shaping of the continental rise by deep geostrophic contour currents. Science 152, 502–508.
Hess, H., Etter, W., 2011. Life and death of *Saccocoma Tenella* (Goldfuss). Swiss Geological Society. https://doi.org/10.1007/s00015-011-0059-z.
Hesselbo, S.P., Deconinck, J.F., Huggett, J.M., Morgans-Bell, H.S., 2009. Late Jurassic palaeoclimatic change from clay mineralogy and gamma-ray spectrometry of the Kimmeridge Clay, Dorset, UK. J. Geol. Soc. 166, 1123–1133.
Hollister, C.D., 1993. The concept of deep-sea contourites. Sediment. Geol. 82, 5–11.
Hollister, C.D., Heezen, B.C., 1972. Geologic effects of ocean bottom currents: Western North Atlantic. In: Gordon, A.L. (Ed.), Studies in Physical Oceanography. Gordon and Breach, New York, pp. 37–66.
Howell, J.A., Schwarz, E., Spalletti, L.A., Veiga, G.D., 2005. The Neuquén Basin: an overview. In: Veiga, G.D., Spalletti, L.A., Howell, J.A., Schwarz, E. (Eds.), The Neuquén Basin, Argentina: A Case Study in Sequence Stratigraphy and Basin Dynamics, vol. 252. Geological Society of London Special Publications, London, pp. 1–14.
Hübscher, C., Dullo, C., Flögel, S., Titschack, J., Schönfeld, J., 2010. Contourite drift evolution and related coral growth in the eastern Gulf of Mexico and its gateways. Int. J. Earth Sci. 99, 191–206.
Hüneke, H., Stow, D.A.V., 2008. Identification of ancient contourites: problems and palaeoceanographic significance. In: Rebesco, M., Camerlenghi, A. (Eds.), Contourites: Developments in Sedimentology, vol. 60. Elsevier, pp. 323–344.
Hunt, D., Tucker, M.E., 1992. Stranded parasequences and the forced regressive wedge systems tract: deposition during base-level fall. Sediment. Geol. 81, 1–9.
Iñigo, J.F., Vargas, R., Novara, E., Pereira, D.M., Schwarz, E., Gardini, M., Gómez, M., Manceda, R., Ayoroa, M.A., Limeres, M., Peroni, G., 2018. La Formación Loma Montosa en el borde nororiental de la Cuenca Neuquina: Análisis secuencial, caracterización paleoambiental y prospectividad remanente. In: Sesiones Generales, 10 Congreso de Exploración y Desarrollo de Hidrocarburos. Instituto Argentino del Petróleo, Mendoza, Argentina, pp. 623–645.
Ito, M., 2002. Kuroshio Current-influenced sandy contourites from the Plio-Pleistocene Kazusa forearc basin, Boso Peninsula, Japan. In: Stow, D.A.V., Pudsey, C.J., Howe, J. A., Faugères, J.-C., Viana, A.R. (Eds.), Deep-Water Contourite Systems: Modern Drifts and Ancient Series, Seismic and Sedimentary Characteristics, vol. 22. Geological Society of London Memoirs, London, pp. 421–432.
Jervey, M.T., 1988. Quantitative geological modeling of siliciclastic rock sequences and their seismic expression. In: Wilgus, C.K., Hastings, B.S., Posamentier, H., Van Wagoner, J., Ross, C.A., Kendall, C.G. (Eds.), Sea-Level Changes—An Integrated Approach, vol. 42. SEPM Special Publication, pp. 47–69.
Johnson, K.S., Paull, C.K., Barry, J.P., Chavez, F.P., 2001. A decadal record of underflows from a coastal river into the deep sea. Geology 29, 1019–1022.
Kietzmann, D.A., Palma, R.M., 2009a. Tafofacies y biofacies de Formación Vaca Muerta en el sector surmendocino de la Cuenca Neuquina: implicancias paleoecológicas. Sedimentol. Estratigr.: Ameghiniana 46, 321–343.
Kietzmann, D.A., Palma, R.M., 2009b. Microcrinoideos saccocómidos en el Tithoniano de la Cuenca Neuquina. ¿Una presencia inesperada fuera de la región del Tethys? Ameghiniana 46, 695–700.
Kietzmann, D.A., Palma, R.M., 2011. Las tempestitas peloidales de la Formación Vaca Muerta (Tithoniano-Valanginiano) en el sector surmendocino de la Cuenca Neuquina. Argentina: Lat. Am. J. Sedimentol. Basin Anal. 18, 121–149.
Kietzmann, D.A., Palma, R.M., Bressan, G.S., 2008. Facies y microfacies de la rampa tithoniana-berriasiana de la Cuenca Neuquina (Formación Vaca Muerta) en la sección del Arroyo Loncoche-Malargüe, provincia de Mendoza. Rev. Asoc. Geol. Argent. 63, 696–713.
Kietzmann, D.A., Palma, R.M., Riccardi, A.C., Martín-Chivelet, J., López-Gómez, J., 2014a. Sedimentology and sequence stratigraphy of a Tithonian–Valanginian carbonate ramp (Vaca Muerta Formation): A misunderstood exceptional source rock in the Southern Mendoza area of the Neuquén Basin, Argentina, Mendoza. Sediment. Geol. 302, 64–86.
Kietzmann, D.A., Ambrosio, A.L., Suriano, J., Alonso, S., Vennari, V.V., Aguirre-Urreta, M.B., Depine, G., Repol, D., 2014b. Variaciones de facies de las secuencias basales de la Formación Vaca Muerta en su localidad tipo (Sierra de la Vaca Muerta), Cuenca Neuquina. In: IX Congreso de Exploración y Desarrollo de Hidrocarburos. IAPG, Mendoza, pp. 299–317.
Kietzmann, D.A., Palma, R.M., Iglesia Llanos, M.P., 2015. Cyclostratigraphy of an orbitally-driven Tithonian–Valanginian carbonate ramp succession, Southern Mendoza, Argentina: implications for the Jurassic–Cretaceous boundary in the Neuquén Basin. Sediment. Geol. 315, 29–46.
Kietzmann, D.A., Iglesia Llanos, M.P., Ivanova, D.K., Kohan Martínez, M., Sturlesi, M.A., 2018. Toward a multidisciplinary chronostratigraphic calibration of the Jurassic-Cretaceous transition in the Neuquén Basin. Rev. Asoc. Geol. Argent. 75, 175–187.
Kietzmann, D.A., González Tomassini, F., Smith, T., 2020a. Grain association, petrography, and facies. In: Minisini, D., Fantín, M., Lanusse Noguera, I., Leanza, H. A. (Eds.), Integrated Geology of Unconventionals: the Case of the Vaca Muerta Play, vol. 121. AAPG Memoir, Argentina, pp. 267–296.
Kietzmann, D.A., Llanos, M.P.I., Kohan Martínez, M., 2020b. Orbital controls and high-resolution cyclostratigraphy of Late Jurassic–Early Cretaceous in the Neuquén Basin. In: Kietzmann, D.A., Folguera, A. (Eds.), Opening and Closure of the Neuquén Basin in the Southern Andes. Springer, pp. 211–235.
Kohan Martínez, M., Kietzmann, D.A., Llanos, M.I., Leanza, H.A., Luppo, T., 2018. Magnetostratigraphy and cyclostratigraphy of the Tithonian interval from the Vaca Muerta Formation, southern Neuquén Basin, Argentina. J. S. Am. Earth Sci. 85, 209–228.
Krim, N., Bonnel, C., Tribovillard, N., Imbert, P., Aubourg, C., Riboulleau, A., Bout-Roumazeilles, V., Hoareau, G., Fasentieux, B., 2017. Paleoenvironmental evolution of the southern Neuquén basin (Argentina) during the Tithonian-Berriasian (Vaca Muerta and Picún Leufú Formations): a multi-proxy approach. Bull. Soc. Geol. Fr. 188, 34.
Knapp, L.J., McMillan, J.M., Harris, N.B., 2017. A depositional model for organic-rich Duvernay Formation mudstones. Sediment. Geol. 347, 160–182.
Kuenen, P.H., 1966. Experimental turbidite lamination in a circular flume. J. Geol. 74, 523–545.
Lavaleye, M.S.S., Duineveld, G.C.A., Berghuis, E.M., Kok, A., Witbaard, R., 2002. A comparison between the megafauna communities on the N.W. Iberian and Celtic continental margins – Effects of coastal upwelling? Prog. Oceanogr. 52, 459–476.
Lazar, O.R., Bohacs, K.M., Macquaker, J.H.S., Schieber, J., Demko, T.M., 2015. Capturing key attributes of fine-grained sedimentary rocks in outcrops, cores, and thin sections: Nomenclature and description guidelines. J. Sediment. Res. 85, 230–246.
Leanza, H.A., Zeiss, A., 1994. The "Lithographic Limestones" of Zapala (central Argentina) and their ammonite fauna. Geobios 16, 245–250.
Leanza, H.A., Sattler, F., Martinez, R.S., Carbone, O., 2011. La Formación Vaca Muerta y equivalentes (Jurásico Tardío-Cretácico Temprano) en la Cuenca Neuquina. In: Leanza, H.A., Arregui, C.D., Carbone, O.C., Danieli, J.C., Vallés, J. (Eds.), Relatorio del XVIII Congreso Geológico Argentino: Asociación Geológica Argentina, pp. 113–130. Neuquén.
Leanza, H.A., 1973. Estudio sobre los cambios faciales de los estratos limitrofes Jurasico-Cretacicos entre Loncopue y Picun Leufu, provincia de Neuquén. Revista de la Asociación Geológica Argentina 28, 97–132.
Leanza, H.A., Kietzmann, D.A., Iglesia Llanos, M.P., Kohan Martínez, M., 2020. Stratigraphic context: Cyclostratigraphy, magnetostratigraphy, and seismic stratigraphy. In: Minisini, D., Fantín, M., Lanusse Noguera, I., Leanza, H.A. (Eds.), Integrated Geology of Unconventionals: the Case of the Vaca Muerta Play, vol. 121. AAPG Memoir, Argentina, pp. 39–60.
Legarreta, L., Gulisano, C.A., 1989. Análisis estratigráfico secuencial de la Cuenca Neuquina (Triásico superior-Terciario inferior). In: Chebli, G.A., Spalletti, L.A. (Eds.), Cuencas Sedimentarias Argentinas: INSUGEO, Serie Correlación Geológica, vol. 6, pp. 221–243.
Leonowicz, P., 2013. The significance of mudstone fabric combined with palaeoecological evidence in determining sedimentary processes - An example from the Middle Jurassic of southern Poland. Geol. Q. 57, 243–260.
Li, Z., Schieber, J., 2018. Detailed facies analysis of the Upper Cretaceous Tununk Shale Member, Henry Mountains Region, Utah: Implications for mudstone depositional models in epicontinental seas. Sediment. Geol. 364, 141–159.
Liu, J.P., Li, A.C., Xu, K.H., Velozzi, D.M., Yang, Z.S., Milliman, J.D., DeMaster, D.J., 2006. Sedimentary features of the Yangtze River-derived along-shelf clinoform deposit in the East China Sea. Continent. Shelf Res. 26, 2141–2156.
Lobza, V., Schieber, J., 1999. Biogenic sedimentary structures produced by worms in soupy, soft muds: Observations from the Chattanooga Shale (Upper Devonian) and experiments. J. Sediment. Res. 69, 1041–1049.
Loucks, R.G., Ruppel, S.C., 2007. Mississippian Barnett Shale: Lithofacies and depositional setting of a deep-water shale-gas succession in the Fort Worth Basin, Texas. AAPG bulletin 91, 579–601.
Lüdmann, T., Wiggershaus, S., Betzler, C., Hübscher, C., 2012. Southwest Mallorca Island: a cool-water carbonate margin dominated by drift deposition associated with giant mass wasting. Mar. Geol. 307, 73–87.
Lynn, R.J., Simpson, J.J., 1990. The flow of the undercurrent over the continental borderland off southern California. J. Geophys. Res. Oceans 95, 12995–13008.
Macquaker, J.H.S., Bohacs, K.M., 2007. On the accumulation of mud. Science 318, 1734–1735.
Mángano, M.G., Buatois, L.A., West, R.R., Maples, C.G., 1998. Contrasting behavioral and feeding strategies recorded by tidal-flat bivalve trace fossils from the Upper Carboniferous of eastern Kansas. Palaios 13, 335–351.
Mantziafou, A., Lascaratos, A., 2004. An eddy resolving numerical study of the general circulation and deep-water formation in the Adriatic Sea: Deep Sea Research Part I. Oceanogr. Res. Pap. 51, 921–952.
Martín-Chivelet, J., Fregenal-Martínez, M.A., Chacón, B., 2003. Mid-depth calcareous contourites in the latest Cretaceous of Caravaca (Subbetic Zone, SE Spain). Origin and palaeohydrological significance. Sediment. Geol. 163, 131–146.
Martín-Chivelet, J., Fregenal-Martínez, M.A., Chacón, B., 2008. Traction structures in contourites. In: Rebesco, M., Camerlenghi, A. (Eds.), Contourites: Developments in Sedimentology, vol. 60, pp. 159–182.
Meier, H.E.M., Feistel, R., Piechura, J., Arneborg, L., Burchard, H., Fiekas, V., Golenko, N., Kuzmina, N., Mohrholz, V., Nohr, C., Paka, V.T., 2006. Ventilation of the Baltic Sea deep water: A brief review of present knowledge from observations and models. Oceanologia 48, 133–164.
Milsom, C.V., 1994. *Saccocoma*: a benthic crinoid from the Jurassic Solnhofen Limestone. Palaeontology 37, 121–129. Germany.
Minisini, D., Eldrett, J., Bergman, S.C., Forkner, R., 2018. Chronostratigraphic framework and depositional environments in the organic-rich, mudstone-dominated Eagle Ford Group, Texas, USA. Sedimentology 65, 1520–1557.

Minisini, D., Fryklund, B., Gerali, F., Fantín, M., 2020a. The first economical unconventional play outside North America: Context, history, and "coopetition". In: Minisini, D., Fantín, M., Lanusse Noguera, I., Leanza, H.A. (Eds.), Integrated Geology of Unconventionals: the Case of the Vaca Muerta Play, vol. 121. AAPG Memoir, Argentina, pp. 1–24.

Minisini, D., Desjardins, P., Otharán, G., Paz, M., Kietzmann, D., Eberli, G., Zavala, C., Simo, T., Macquaker, J.H., Heine, C., 2020b. Sedimentology, Depositional Model and Implications for Reservoir Quality. In: Minisini, D., Fantín, M., Lanusse Noguera, I., Leanza, H.A. (Eds.), Integrated Geology of Unconventionals: the Case of the Vaca Muerta Play, vol. 121. AAPG Memoir, Argentina, pp. 201–236.

Miramontes, E., Garreau, P., Caillaud, M., Jouet, G., Pellen, R., Hernández-Molina, F.J., Clare, M.A., Cattaneo, A., 2019. Contourite distribution and bottom currents in the NW Mediterranean Sea: Coupling seafloor geomorphology and hydrodynamic modelling. Geomorphology 333, 43–60.

Mitchum, R.M.J., Uliana, M.A., 1985. Seismic stratigraphy of carbonate depositional sequences, Upper Jurassic-Lower Cretaceous, Neuquén basin, Argentina. In: Berg, O., Woolverton, D. (Eds.), Seismic Stratigraphy II: an Integrated Approach to Hydrocarbon Exploration, vol. 39. AAPG Memoir, Tulsa, pp. 255–274.

Moros, M., Kotilainen, A.T., Snowball, I., Neumann, T., Perner, K., Meier, H.M., Leipe, T., Zillén, L., Damste, J.S.S., Schneider, R., 2020. Is 'deep-water formation'in the Baltic Sea a key to understanding seabed dynamics and ventilation changes over the past 7,000 years? Quat. Int. 550, 55–65.

Mulder, T., 2011. Gravity processes and deposits on continental slope, rise and abyssal plains. In: Hüneke, H., Mulder, T. (Eds.), Deep-Sea Sediments: Developments in Sedimentology, vol. 63. Elsevier, pp. 25–148.

Mulder, T., Faugères, J.-C., Gonthier, E., 2008. Mixed turbidite-contourite systems. In: Rebesco, M., Camerlenghi, A. (Eds.), Contourites: Developments in Sedimentology, vol. 60. Elsevier, pp. 435–456.

Myrow, P.M., Southard, J.B., 1996. Tempestite deposition. J. Sediment. Res. 66, 875–887.

Noffke, N., 2010. Geobiology: Microbial Mats in Sandy Deposits from the Archaean Era to Today. Springer, Heidelberg, p. 194.

Notta, R., Davogustto, O., Desjardins, P., Williams, B., 2017. Slumps deposits identification in low angle carbonate ramp settings, Cruz de Lorena (Neuquén Basin, Argentina): Towards an integrated model explaining anomalous water recovery and poor well performance. In: XX Congreso Geológico Argentino, Simposio 5 Geología de la Formación Vaca Muerta: Asociación Geológica Argentina, pp. 91–96. Tucumán.

Notta, R., Kruijs, E., Jain, V., Diaz-Perez, G., Mandler, H., 2020. De-risking the Sierras Blancas and Cruz de Lorena blocks, black-oil window. In: Minisini, D., Fantín, M., Lanusse Noguera, I., Leanza, H.A. (Eds.), Integrated Geology of Unconventionals: the Case of the Vaca Muerta Play, vol. 121. AAPG Memoir, Argentina, pp. 445–468.

Nyhuis, C.J., Rippen, D., Denayer, J., 2014. Facies characterization of organic-rich mudstones from the Chokier Formation (lower Namurian), south Belgium. Geol. Belg. 17, 311–322.

O'Brien, N.R., 1996. Shale lamination and sedimentary processes. In: Kemp, A.E.S. (Ed.), Palaeoclimatology and Palaeoceanography from Laminated Sediments, vol. 116. Geological Society of London Special Publications, London, pp. 23–36.

Oczlon, M.S., Balda, M.A.D., 1992. Contourites in laminated black shale facies of the Aldeatejada Formation (Precambian/Cambrian boundary range, province of Salamanca, Western Spain). Rev. Soc. Geol. Espana 5, 167–176.

Olivero, E.B., López-Cabrera, M.I., 2010. *Tasselia ordamensis*: A biogenic structure of probable deposit-feeding and gardening maldanid polychaetes. Palaeogeogr. Palaeoclimatol. Palaeoecol. 292, 336–348.

Otharán, G.A., Zavala, C., Arcuri, M., Di Meglio, M., Zorzano, A., Marchal, D., Köhler, G., 2020. Facies analysis of fine-grained deposits related to muddy underflows. Vaca Muerta Formation (Tithonian-Valanginian), central Neuquen Basin, Argentina. Andean Geol. 47, 384–417.

Palanques, A., Durrieu de Madron, X., Puig, P., Fabres, J., Guillén, J., Calafat, A., Canals, M., Heussner, S., Bonnin, J., 2006. Suspended sediment fluxes and transport processes in the Gulf of Lions submarine canyons. The role of storms and dense water cascading. Mar. Geol. 234, 43–61.

Parada, M.N., 2019. Análisis Sedimentológico e Icnológico de la Sección Basal de la Formación Picún Leufú (Tithoniano-Berriasiano) en su Localidad Tipo, Cuenca Neuquina, Argentina. Bachelor's tesis. Universidad Nacional de Río Negro, General Roca, p. 48.

Parsons, J.D., Bush, J.W.M., Syvitski, J.P.M., 2001. Hyperpycnal plume formation from riverine outflows with small sediment concentrations. Sedimentology 48, 465–478.

Paz, M., 2021. Sedimentology, Ichnology and Sequence Stratigraphy of Black Shales from the Upper Jurassic – Lower Cretaceous Vaca Muerta Formation, Neuquén Basin, Argentina. Ph.D thesis. University of Saskatchewan, Saskatoon, Canada, p. 455.

Paz, M., Ponce, J.J., Buatois, L.A., Mángano, M.G., Carmona, N.B., Pereira, E., Desjardins, P.R., 2019. Bottomset and foreset sedimentary processes in the mixed carbonate-siliciclastic Upper Jurassic-Lower Cretaceous Vaca Muerta Formation, Picún Leufú Area, Argentina. Sediment. Geol. 389, 161–185.

Paz, M., Ponce, J.J., Mángano, M.G., Buatois, L.A., Carmona, N.B., Wetzel, A., Pereira, E., Rodríguez, M.N., 2021. The Vaca Muerta transgression (Upper Jurassic), Neuquén Basin, Argentina: Insights into the evolution and timing of aeolian–marine transitions. Sedimentology 68, 2732–2764.

Paz, M., Mángano, M.G., Buatois, L.A., Desjardins, P.R., Notta, R., González Tomassini, F. G., Carmona, N.B., 2022. Ichnology of muddy shallow-water contourites from the Upper Jurassic-Lower Cretaceous Vaca Muerta Formation, Argentina: Implications for trace-fossil models. Palaios 37, 1–18.

Pellegrini, C., Maselli, V., Trincardi, F., 2016. Pliocene–Quaternary contourite depositional system along the south-western Adriatic margin: changes in sedimentary stacking pattern and associated bottom currents. Geo Mar. Lett. 36, 67–79.

Pemberton, S.G., Frey, R.W., 1982. Trace fossil nomenclature and the *Planolites-Palaeophycus* dilemma. J. Paleontol. 56, 843–881.

Pomar, L., Molina, J.M., Ruiz-Ortiz, P.A., Vera, J.A., 2019. Storms in the deep: Tempestite- and beach-like deposits in pelagic sequences (Jurassic, Subbetic, South of Spain). Mar. Petrol. Geol. 107, 365–381.

Ponce, J.J., Olivero, E.B., Martinioni, D.R., López Cabrera, M.I., 2007. Sustained and episodic gravity-flow deposits and related bioturbation patterns in Paleogene turbidites (Tierra del Fuego, Argentina). In: Bromley, R.G., Buatois, L.A., Mángano, M.G., Genise, J.F., Melchor, R.N. (Eds.), Sediment-Organism Interactions: A Multifaceted Ichnology, vol. 88. SEPM Special Publication, pp. 253–266.

Ponce, J.J., Carmona, N.B., Montagna, A., Canale, N., 2015. Sedimentología e icnología de los sistemas petroleros no convencionales de la Cuenca Neuquina. Guia de Campo: Universidad Nacional de Río Negro - Fundación YPF, General Roca, p. 114.

Pose, F., Gangui, A., Galeazzi, S., 2014. Estratigrafía secuencial del intervalo Quintuco-Vaca Muerta en el Engolfamiento Neuquino, Cuenca Neuquina, Argentina. In: Simposio de Recursos No Convencionales, IX Congreso de Exploración y Desarrollo de Hidrocarburos. IAPG, Mendoza, pp. 211–229.

Puig, P., Ogston, A.S., Guillén, J., Fain, A.M.V., Palanques, A., 2007. Sediment transport processes from the topset to the foreset of a crenulated clinoform (Adriatic Sea). Continent. Shelf Res. 27, 452–474.

Pratt, L.M., 1984. Influence of paleoenvironmental factors on preservation of organic matter in Middle Cretaceous Greenhorn Formation, Pueblo, Colorado. American Association of Petroleum Geologists Bulletin 68, 1146–1159.

Puig, P., Greenan, B.J.W., Li, M.Z., Prescott, R.H., Piper, D.J.W., 2013. Sediment transport processes at the head of Halibut Canyon, eastern Canada margin: An interplay between internal tides and dense shelf-water cascading. Mar. Geol. 341, 14–28.

Ramsay, P.J., 1994. Marine geology of the Sodwana Bay shelf, southeast Africa. Mar. Geol. 120, 225–247.

Rebesco, M., Hernández-Molina, F.J., Van Rooij, D., Wåhlin, A., 2014. Contourites and associated sediments controlled by deep-water circulation processes: State-of-the-art and future considerations. Mar. Geol. 352, 111–154.

Reijenstein, H.M., Domínguez, R.F., Bande, A., Vallejo, M.D., Notta, R., Guerberoff, D., Lanusse, I., Köhler, G., Borgnia, M., Benoit, S., Leanza, H.A., Gómez Rivarola, L., Weger, R., González Tomassini, F., Kietzmann, D., Rodríguez Schelotto, M.L., Desjardins, P., Marchal, D., Martínez, A., Vittore, F., Fantín, M., Depine, G., Sattler, F., Rosemblat, A., 2017. Transecta sísmica regional del sistema Vaca Muerta – Quintuco: Interpretación de facies sísmicas basada en impedancia acústica y litofacies dominantes. In: XX Congreso Geológico Argentino, Simposio 5 Geología de la Formación Vaca Muerta: Asociación Geológica Argentina, pp. 130–134. Tucumán.

Reijenstein, H.M., Posamentier, H.W., Bande, A., Lozano, F.P., Domínguez, R.F., Wilson, R., Catuneanu, O., Galeazzi, S., 2020. Seismic geomorphology, depositional elements, and clinoform sedimentary processes: Impact on unconventional reservoir prediction. In: Minisini, D., Fantín, M., Lanusse Noguera, I., Leanza, H.A. (Eds.), Integrated Geology of Unconventionals: the Case of the Vaca Muerta Play, vol. 121. AAPG Memoir, Argentina, pp. 237–266.

Reineck, H.-E., 1963. Sedimentgefüge im Bereich der südliche Nordsee. Abhandlungen Senckenbergischen Naturforsche de Gesellschaft 505, 1–138.

Reisdorf, A.G., Anderson, G.S., Bell, L.S., Klug, C., Schmid-Röhl, A., Röhl, H.J., Jung, M., Wuttke, M., Maisch, M.W., Benecke, M., Wyler, D., Bux, R., Fornaro, P., Wetzel, A., 2014. Reply to "Ichthyosaur embryos outside the mother body: not due to carcass explosion but to carcass implosion" by van Loon. Palaeobiodivers. Palaeoenviron. 94, 487–494, 2013.

Repol, D., Desjardins, P.R., Buenafama, P., Li, X., Depine, G., Thompson, M., Rucci, F., Veldkamp, J., Smith, P., 2014. Vaca Muerta liquid-rich shale: Key properties and insights towards a predictive geological model, Sierras Blancas block, Neuquén Basin. In: Actas IX Congreso de Exploración y Desarrollo de Hidrocarburos. Simposio de Recursos No Convencionales, IAPG, Mendoza, pp. 567–586.

Ribó, M., Puig, P., Muñoz, A., Iacono, C.L., Masqué, P., Palanques, A., Acosta, J., Guillén, J., Ballesteros, M.G., 2016. Morphobathymetric analysis of the large fine-grained sediment waves over the Gulf of Valencia continental slope (NW Mediterranean). Geomorphology 253, 22–37.

Robinson, R.S., Murillo de Nava, J.M., Gorsline, D.S., 2007. Slope currents and contourites in an eastern boundary current regime: California Continental Borderland. In: Viana, A.R., Rebesco, M. (Eds.), Economic and Palaeoceanographic Significance of Contourite Deposits, vol. 276. Geological Society of London Special Publications, pp. 155–169.

Rodríguez Blanco, L., Eberli, G.P., Weger, R.J., Swart, P.K., Tenaglia, M., Rueda Sanchez, L.E., McNeill, D.F., 2020. Periplatform ooze in a mixed siliciclastic-carbonate system - Vaca Muerta Formation, Argentina. Sediment. Geol. 396, 1–17.

Rodríguez-Tovar, F.J., Hernández-Molina, F.J., 2018. Ichnological analysis of contourites: Past, present and future. Earth Sci. Rev. 182, 28–41.

Rodríguez-Tovar, F.J., Hernández-Molina, F.J., Hüneke, H., Llave, E., Stow, D., 2019. Contourite facies model: Improving contourite characterization based on the ichnological analysis. Sediment. Geol. 384, 60–69.

Ruffell, A.H., Price, G.D., Mutterlose, J., Kessels, K., Baraboshkin, E., Gröcke, D.R., 2002. Palaeoclimate indicators (clay minerals, calcareous nannofossils, stable isotopes) compared from two successions in the late Jurassic of the Volga Basin (SE Russia). Geol. J. 37, 17–33.

Sagasti, G., 2005. Hemipelagic record of orbitally-induced dilution cycles in Lower Cretaceous sediments of the Neuquén Basin. In: Veiga, G.D., Spalletti, L.A., Howell, J.A., Schwarz, E. (Eds.), The Neuquén Basin, Argentina: A Case Study in Sequence Stratigraphy and Basin Dynamics, vol. 252. Geological Society of London, Special Publications, pp. 231–250.

Sato, T., Taniguchi, K., Takagawa, T., Masuda, F., 2011. Generation of tidal bedding in a circular flume experiment: Formation process and preservation potential of mud drapes. Geo Mar. Lett. 31, 101–108.
Sattler, F., Domínguez, R.F., Benoit, S., Marchal, D., 2016. Anexo 1. In: González, G., Vallejo, M.D., Kietzmann, D.A., Marchal, D., Desjardins, P.R., González Tomassini, F., Gómez Rivarola, L., Domínguez, R.F., Fantín, M.A. (Eds.), Transecta Regional de la Formación Vaca Muerta–Integración de Sísmica, Registros de Pozos, Coronas y Afloramientos. IAPG, Buenos Aires.
Scasso, R.A., Alonso, M.S., Lanés, S., Villar, H.J., Lippai, H., 2002. Petrología y geoquímica de una ritmita marga-caliza del Hemisferio Austral: El Miembro Los Catutos (Formación Vaca Muerta), Tithoniano medio de la Cuenca Neuquina. Rev. Asoc. Geol. Argent. 57, 143–159.
Scherer, C.M., Mello, R.G., Ferronatto, J.P., Amarante, F.B., Reis, A.D., Souza, E.G., Goldberg, K., 2020. Changes in prevailing surface-palaeowinds of western Gondwana during Early Cretaceous. Cretac. Res. 116, 104598.
Schieber, J., 1994. Evidence for high-energy events and shallow-water deposition in the Chattanooga Shale, Devonian, central Tennessee, USA. Sediment. Geol. 93, 193–208.
Schieber, J., 1999. Distribution and deposition of mudstone facies in the Upper Devonian Sonyea Group of New York. J. Sediment. Res. 69, 909–925.
Schieber, J., 2011. Reverse engineering mother nature - Shale sedimentology from an experimental perspective. Sediment. Geol. 238, 1–22.
Schieber, J., 2016. Mud re-distribution in epicontinental basins - Exploring likely processes. Mar. Petrol. Geol. 71, 119–133.
Schieber, J., Southard, J.B., 2009. Bedload transport of mud by floccule ripples—direct observation of ripple migration processes and their implications. Geology 7, 483–486.
Schieber, J., Southard, J.B., Thaisen, K.G., 2007. Accretion of mudstone beds from migrating floccule ripples. Science 318, 1760–1763.
Shanmugam, G., Spalding, T.D., Rofheart, D.H., 1993a. Process sedimentology and reservoir quality of deep-marine bottom- current reworked sands (sandy contourites): an example from the Gulf of Mexico. Am. Assoc. Petrol. Geol. Bullet. 77, 1241–1259.
Shanmugam, G., Spalding, T.D., Rofheart, D.H., 1993b. Traction structures in deep-marine, bottom-current - reworked sands in the Pliocene and Pleistocene. Gulf Mex.: Geology 21, 929–932.
Shanmugam, G., 2006. Deep-Water Processes and Facies Models: Implications for Sandstone Petroleum Reservoirs. Elsevier, Amsterdam, p. 476.
Shanmugam, G., 2013. Comment on "Internal waves, an under-explored source of turbulence events in the sedimentary record" by L. Pomar, M. Morsilli, P. Hallock, and B. Bádenas [Earth-Science Reviews, 111 (2012), 56–81]. Earth-Science Reviews 116, 195–205.
Shanmugam, G., 2017. The contourite problem. In: Mazumder, R. (Ed.), Sediment Provenance: Influences on Compositional Change from Source to Sink. Elsevier, Cambridge, pp. 183–254.
Sholkovitz, E., Soutar, A., 1975. Changes in the composition of the bottom water of the Santa Barbara Basin: effect of turbidity currents. Deep-Sea Res. 22, 13–21.
Singh, P., Slatt, R.M., Coffey, W., 2008. Barnett Shale - unfolded: sedimentology, sequence stratigraphy, and regional mapping. Gulf Coast Assoc. Geol. Soc. Trans. 58, 777–795.
Sivkov, V., Gorbatskiy, V., Kuleshov, A., Zhurov, Y., 2002. Muddy contourites in the Baltic Sea: an example of a shallow-water contourite system. In: Stow, D.A.V., Pudsey, C.J., Howe, J.A., Faugères, J.-C., Viana, A.R. (Eds.), Deep-Water Contourite Systems: Modern Drifts and Ancient Series, Seismic and Sedimentary Characteristics, vol. 22. Geological Society of London Memoirs, London, pp. 121–136.
Spalletti, L.A., Gasparini, Z., Veiga, G., Schwarz, E., Fernandez, M., Matheos, S., 1999. Facies anóxicas, procesos deposicionales y herpetofauna de la rampa marina Titoniano-Berriasiana en la Cuenca Neuquina (Yesera del Tromen), Neuquén, Argentina. Rev. Geol. Chile 26, 109–123.
Spalletti, L.A., Franzese, J.R., Matheos, S.D., Schwarz, E., 2000. Sequence stratigraphy of a tidally dominated carbonate-siliciclastic ramp; the Tithonian-Early Berriasian of the Southern Neuquén Basin, Argentina. J. Geol. Soc. Lond. 157, 433–446.
Spalletti, L.A., Arregui, C.D., Veiga, G.D., 2011. La Formación Tordillo y equivalentes (Jurásico Tardío) en la cuenca Neuquina. In: Leanza, H.A., Arregui, C.D., Carbone, O. C., Danieli, J.C., Vallés, J. (Eds.), Relatorio del XVIII Congreso Geológico Argentino: Asociación Geológica Argentina, pp. 99–112. Buenos Aires.
Stanley, D.J., 1993. Model for turbidite-to-contourite continuum and multiple process transport in deep marine settings: examples in the rock record. Sediment. Geol. 82, 241–255.
Stipanicic, P.N., 1969. El avance en los conocimientos del Jurásico argentino a partir del esquema de Groeber. Rev. Asoc. Geol. Argent. 24, 367–388.
Stow, D.A.V., Bowen, A.J., 1980. A physical model for the transport and sorting of fine-grained sediment by turbidity currents. Sedimentology 27, 31–46.
Stow, D.A.V., Faugères, J.-C., 2008. Contourite facies and the facies model. In: Rebesco, M., Camerlenghi, A. (Eds.), Contourites: Developments in Sedimentology, vol. 60, pp. 223–256.
Stow, D.A.V., Lovell, J.P.B., 1979. Contourites: Their recognition in modern and ancient sediments. Earth Sci. Rev. 14, 251–291.
Stow, D.A.V., Shanmugam, G., 1980. Sequence of structures in fine-grained turbidites: Comparison of recent deep-sea and ancient flysch sediments. Sediment. Geol. 25, 23–42.
Stow, D., Smillie, Z., 2020. Distinguishing between deep-water sediment facies: Turbidites, contourites and hemipelagites. Geosciences 10, 68.
Stow, D.A.V., Faugères, J.-C., Viana, A.R., Gonthier, E., 1998. Fossil contourites: A critical review. Sediment. Geol. 115, 3–31.
Stratford, K., Williams, R.G., Myers, P.G., 2000. Impact of the circulation on sapropel formation in the eastern Mediterranean. Global Biogeochem. Cycles 14, 683–695.
Talling, P.J., 2014. On the triggers, resulting flow types and frequencies of subaqueous sediment density flows in different settings. Mar. Geol. 352, 155–182.
Taylor, A.M., Goldring, R., 1993. Description and analysis of bioturbation and ichnofabric. J. Geol. Soc. Lond. 150, 141–148.
Trabucho-Alexandre, J., Dirkx, R., Veld, H., Klaver, G., de Boer, P.L., 2012. Toarcian black shales in the Dutch Central Graben: Record of energetic, variable depositional conditions during an Oceanic Anoxic Event. J. Sediment. Res. 82, 104–120.
Traykovski, P., Geyer, W.R., Irish, J.D., Lynch, J.F., 2000. The role of wave-induced density-driven fluid mud flows for cross-shelf transport on the Eel River continental shelf. Continent. Shelf Res. 20, 2113–2140.
Tucholke, B.E., 2002. The Greater Antilles Outer Ridge: development of a distal sedimentary drift by deposition of fine-grained contourites. In: Stow, D.A., Pudsey, C.J., Howe, J.A., Faugeres, J.-C., Viana, A.R. (Eds.), Deep-Water Contourite Systems: Modern Drifts and Ancient Series, Seismic and Sedimentary Characteristics, vol. 22. The Geological Society of London, pp. 39–55.
Tunik, M., Folguera, A., Naipauer, M., Pimentel, M., Ramos, V.A., 2010. Early uplift and orogenic deformation in the Neuquén Basin: Constraints on the Andean uplift from U-Pb and Hf isotopic data of detrital zircons. Tectonophysics 489, 258–273.
Urgeles, R., Cattaneo, A., Puig, P., Liquete, C., De Mol, B., Amblàs, D., Sultan, N., Trincardi, F., 2011. A review of undulated sediment features on Mediterranean prodeltas: distinguishing sediment transport structures from sediment deformation. Mar. Geophys. Res. 32, 49–69.
Vandorpe, T.P., van Rooij, D., Stow, D.A.V., Henriet, J.P., 2011. Pliocene to Recent shallow-water contourite deposits on the shelf and shelf edge off south-western Mallorca, Spain. Geo Mar. Lett. 31, 391–403.
Verdicchio, G., Trincardi, F., 2008a. Mediterranean shelf-edge muddy contourites: Examples from the Gela and South Adriatic basins. Geo Mar. Lett. 28, 137–151.
Verdicchio, G., Trincardi, F., 2008b. Shallow-water contourites. In: Rebesco, M., Camerlenghi, A. (Eds.), Contourites: Developments in Sedimentology, vol. 60, pp. 409–433.
Viana, A.R., Faugères, J.C., Kowsmann, R.O., Lima, J.A.M., Caddah, L.F.G., Rizzo, J.G., 1998. Hydrology, morphology and sedimentology of the Campos continental margin, offshore Brazil: Sediment. Geol. 115, 133–157.
Viana, A.R., De Almeida, W., De Almeida, C.W., 2002. Upper slope sands: Late Quaternary shallow-water sandy contourities of Campos Basin, SW Atlantic Margin. In: Stow, D.A.V., Pudset, C.J., Howe, J.A., Faugères, J.-C., Viana, A.R. (Eds.), Deep-Water Contourite Systems: Modern Drifts and Ancient Series, vol. 22. Geological Society of London Memoirs, London, pp. 261–270.
Volkheimer, W., Rauhut, O.W., Quattrocchio, M.E., Martinez, M.A., 2008. Jurassic paleoclimates in Argentina, a review. Rev. Asoc. Geol. Argent. 63, 549–556.
Wagner, T., Hofmann, P., Flögel, S., 2013. Marine black shale deposition and Hadley Cell dynamics: A conceptual framework for the Cretaceous Atlantic Ocean. Mar. Petrol. Geol. 43, 222–238.
Warrick, J.A., Milliman, J.D., 2003. Hyperpycnal sediment discharge from semiarid southern California rivers: Implications for coastal sediment budgets. Geology 31, 781–784.
Wells, M.R., Allison, P.A., Hampson, G.J., Piggott, M.D., Pain, C.C., 2005. Modelling ancient tides: the Upper Carboniferous epi-continental seaway of Northwest Europe. Sedimentology 52, 715–735.
Wetzel, A., Bromley, R.G., 1996. The ichnotaxon *Tasselia ordamensis* and its junior synonym *Caudichnus annulatus*. J. Paleontol. 70, 523–526.
Wetzel, A., Werner, F., Stow, D.A.V., 2008. Bioturbation and biogenic sedimentary structures in contourites. In: Rebesco, M., Camerlenghi, A. (Eds.), Contourites: Developments in Sedimentology, vol. 60, pp. 183–202.
Wheatcroft, R.A., Smith, C.R., Jumars, P.A., 1989. Dynamics of surficial trace assemblages in the deep sea. Deep Sea Research Part A. Oceanogr. Res. Pap. 36, 71–91.
Wignall, P.B., Myers, K.J., 1988. Interpreting benthic oxygen levels in mudrocks: A new approach. Geology 16, 452–455.
Wilson, R.D., Schieber, J., 2014. Muddy prodeltaic hyperpycnites in the Lower Genesee Group of Central New York, USA: Implications for mud transport in epicontinental seas. J. Sediment. Res. 84, 866–874.
Witzke, B.J., 1987. Models for circulation patterns in epicontinental seas applied to Paleozoic facies of North America craton. Paleoceanography 2, 229–248.
Wright, V.P., 1992. A revised classification of limestones. Sediment. Geol. 76, 177–185.
Wright, L.D., Friedrichs, C.T., Kim, S.C., Scully, M.E., 2001. Effects of ambient currents and waves on gravity-driven sediment transport on continental shelves. Mar. Geol. 175, 25–45.
Yawar, Z., Schieber, J., 2017. On the origin of silt laminae in laminated shales. Sediment. Geol. 360, 22–34.
Zeller, M., 2013. Facies, Geometries and Sequence Stratigraphy of the Mixed Carbonate - Siliciclastic Quintuco - Vaca Muerta System in the Neuquen Basin, Argentina: An Integrated Approach. University of Miami, Ph.D Thesis, p. 206.
Zeller, M., Verwer, K., Eberli, G.P., Massaferro, J.L., Schwarz, E., Spalletti, L.A., 2015. Depositional controls on mixed carbonate-siliciclastic cycles and sequences on gently inclined shelf profiles. Sedimentology 62, 2009–2037.